Istituto Nazionale di Geofisica e Vulcanologia

SUMMARY REPORT ON THE 30 OCTOBER, 2016 EARTHQUAKE IN CENTRAL ITALY M_w 6.5

Gruppo di Lavoro INGV sul Terremoto in centro Italia

10 November 2016

Cite as: *Gruppo di Lavoro INGV sul terremoto in centro Italia (2016). Summary report on the October 30, 2016 earthquake in central Italy M_w 6.5, doi: 10.5281/zenodo.166238*

INDEX

1. Introduction ***3***

1.1 Historical seismicity *5*

1.2 Instrumental seismicity *7*

1.3 Active faults *8*

1.4 Seismic networks *11*

2. Main Event ***12***

2.1 Focal mechanism *12*

2.2 Strong Motion Data *14*

2.3 ShakeMap *18*

2.4 Did you feel the earthquake? *20*

2.5 Source models by Strong Motion data *23*

2.6 Propagation of seismic waves in a 3D velocity model *25*

2.7 Source models from GPS data *26*

2.8 Source Models for SAR data *29*

2.9 Surface faulting *34*

3. Earthquakes Sequence ***39***

3.1 Space-temporal pattern of the sequence *39*

3.2 The fault system imaged by earthquakes distribution: refined locations *40*

3.3 Short-term earthquake forecast (OEF) for the Amatrice-Norcia sequence (November 9, 2016) *43*

References ***45***

1. Introduction

The earthquake of October 30th 2016 at 06:40:17 UTC, (07:40:17, Italian time) was the Italian strongest event after the 1980 M_W 6.9 Irpinia earthquake. The hypocenter coordinates are: Latitude 42.84 North, Longitude 11.13 East, depth 9 km. The magnitude calculated in the INGV monitoring room is 6.1 M_L e 6.5 M_W.
The earthquake affected the provinces of Perugia, Rieti and Macerata and was strongly felt in central Italy; the epicenter is located 5 km from Norcia, 7 from Castelsantangelo sul Nera and Preci, 10 from Visso. In case of an earthquake of magnitude 6.5 the fault has an area of several hundred square kilometers and therefore the entire area above and around the fault is affected by strong shaking.
Up to this moment the earthquake of October 30 is the strongest event of the sequence which began with the earthquake of August 24th of M_W=6.0 and also counts a quake of magnitude M_W=5.9 of October 26th.

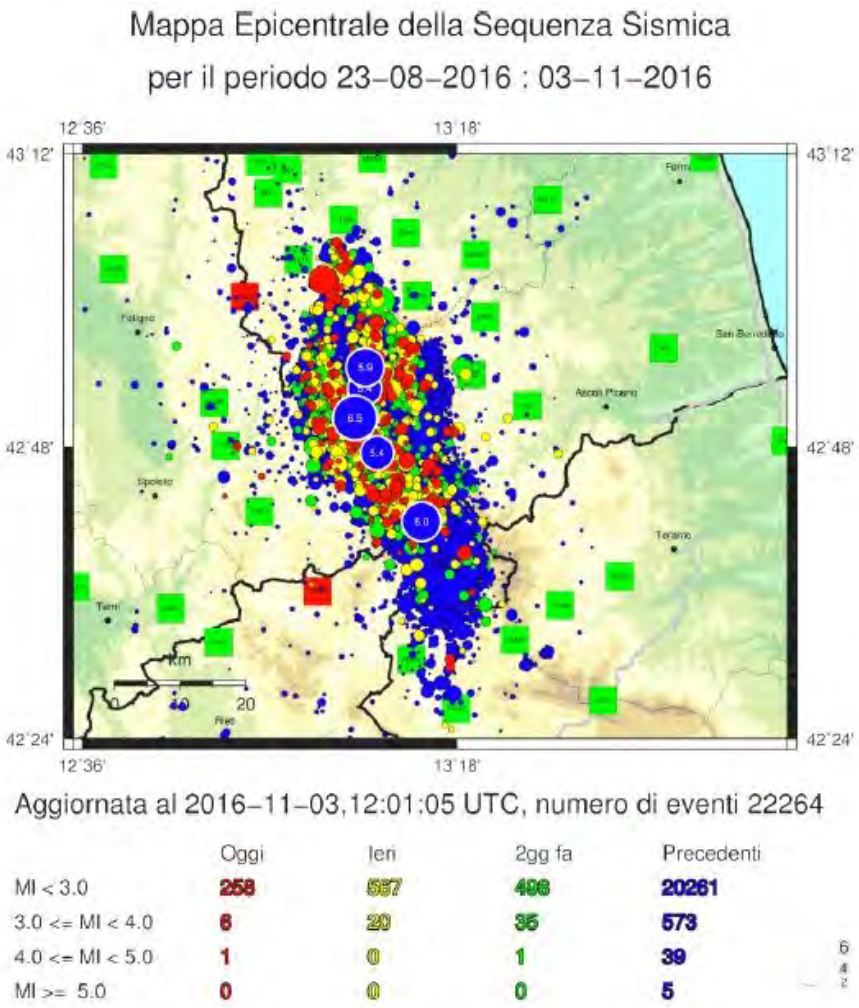

The area affected by the aftershocks stretches for about 40 km, from Accumoli to the South to Visso in the North. It overlays to the northern part of the fault system that was activated by the earthquake of August 24, and also affects the southern part of the structure affected by the October 26th quake.

Figure 1.1 - Epicentral map of the seismic sequence up to 03/11/2016. The total number of epicentres from august 24th 2016 is 22264. Red symbols are events on November 3rd, yellow ones are November 2nd, green November 1st and blu previous ones.

Below we show the seismogram of CESX broadband seismic station, (located at Cesi, municipality of Terni) of the INGV National Seismic Network, of 30th October 2016. It is possible to distinguish the arrival of seismic waves at 6:40 UTC (7:40 Italian time) of the large earthquake of 6.5 M_W. The large number of events that followed the main shock is clearly visible.

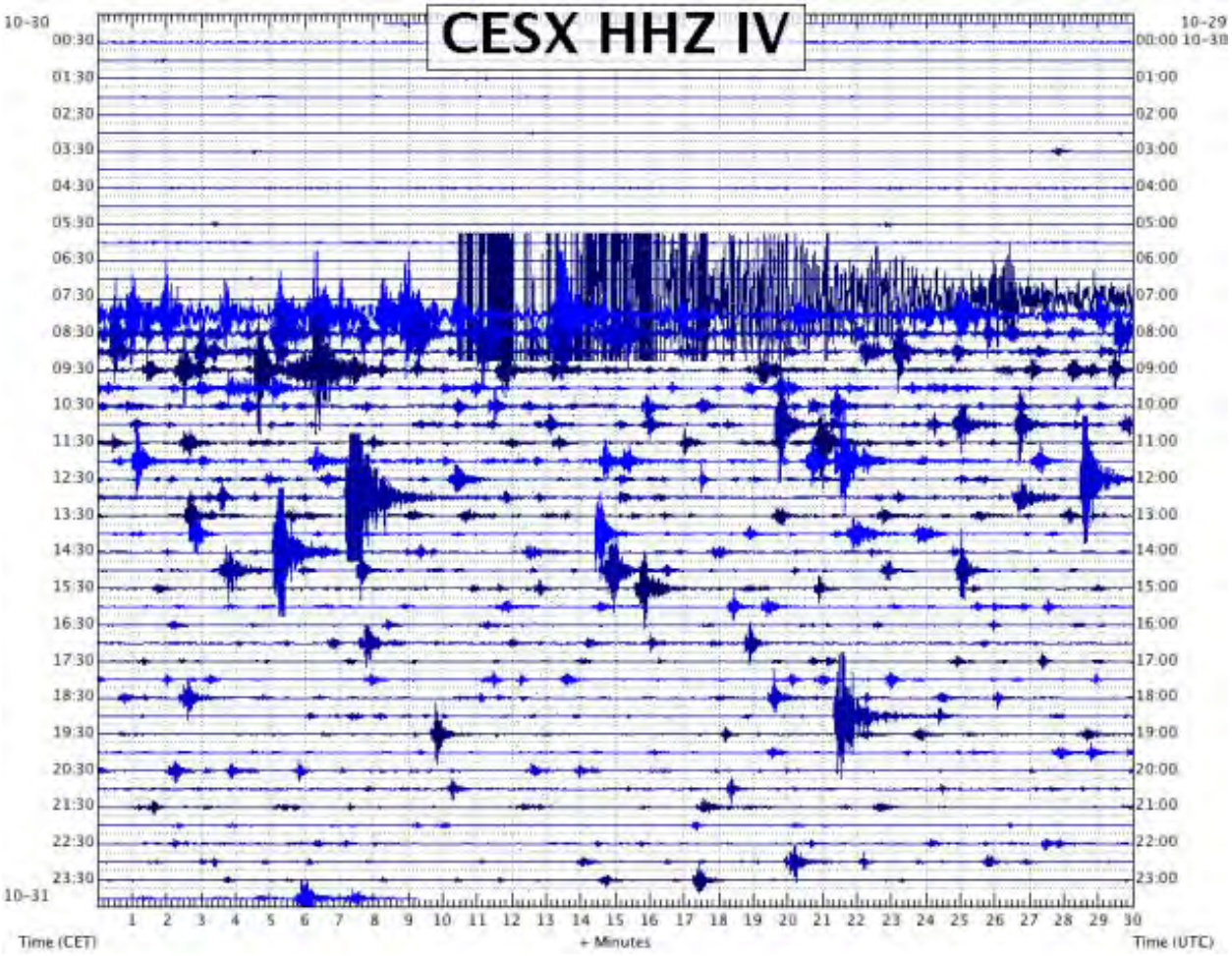

Figure 1.2 - Daily seismogram of the seismic station CESX Cesi, Terni, each line is 30 minutes; It is clearly visible the main earthquake of 6:40 UTC.

1.1 Historical seismicity

The main events of the ongoing Monti della Laga-Valnerina seismic sequence occurred in a territory that was affected by relevant earthquakes in the past. Some of these historical earthquakes occurred within sequences, none of which seem quite comparable with the current one.

On the whole, the seismic history of the Monti della Laga-Valnerina area is comparatively well known. However, in some sectors of this area much less information is available than in others and the features of seismicity in each sector are noticeably different.

In the Amatrice sector – where the major effects of the August 24 earthquake took place - the most distinctive feature is a cluster of four earthquakes occurred in: 1627 (Accumoli, Io 7-8 MCS, M_W 5.3); 1639 (Amatrice, Io 9-10 MCS, M_W 6.2); 1646 (Monti della Laga, Io 9 MCS, M_W 5.9) and 1672 (Amatrice, Io 7-8 MCS, M_W 5.3). The 1639 earthquake laid waste to Amatrice and the surrounding villages.

In Valnerina, the earthquakes located closest to the epicentre of the October 30 main event are those of 1328 (Valnerina, Io 10 MCS, M_W 6.5); 1719 (Valnerina, Io 8 MCS, M_W 5.6); 1730 (Valnerina, Io 9 MCS, M_W 6) and 1859 (Valnerina, Io 8-9 MCS, M_W 5.7).

In the Visso-Ussita-Castelsantangelo sul Nera area the intensity degrees now being assessed for the October 26 events appear very likely to be the historical maximum for this sector, at the current state of knowledge.

The ongoing sequence cannot be compared with the long and complex sequence of the year 1703 (January 14, Valnerina, Io 11, M_W 6.9; February 2, Aquilano, Io 10, M_W 6.7), unquestionably the historical maximum on record for the whole area, that had a considerably worse and much more widespread impact than what is emerging in the present situation.

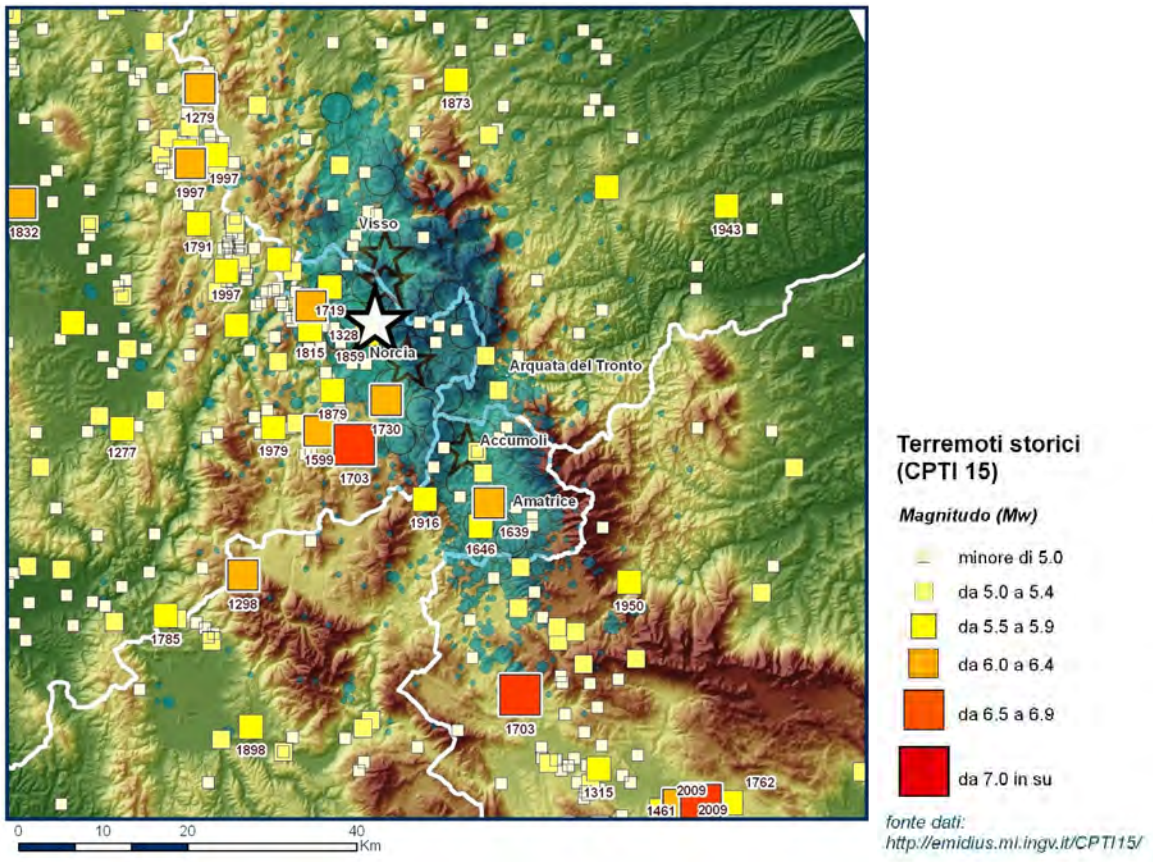

Figure 1.1.1 - Map of the historical earthquakes in the region.

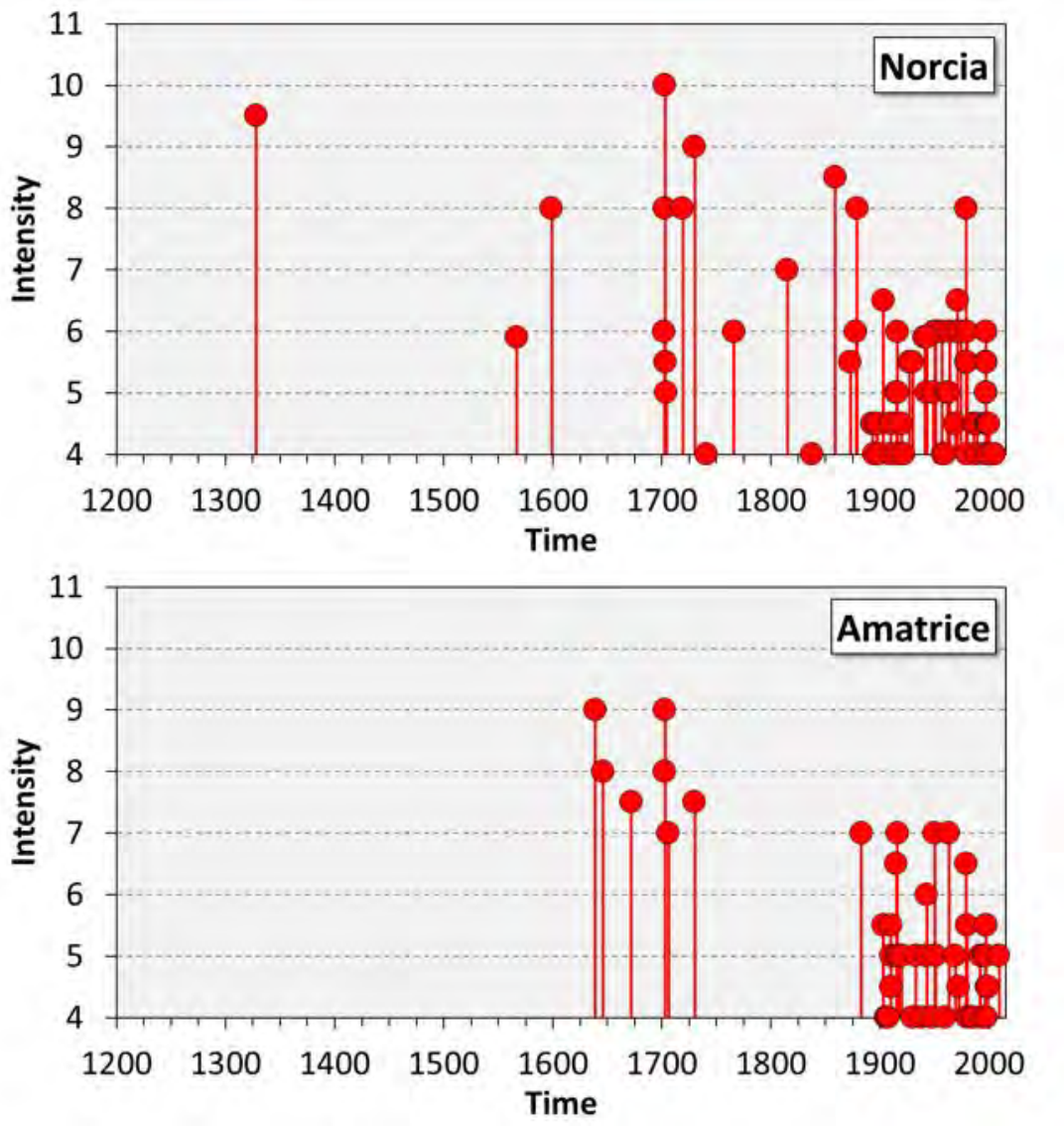

Figure 1.1.2 - Comparison between seismic histories in Norcia and Amatrice [http://emidius.mi.ingv.it/CPTI15-DBMI15/].

1.2 Instrumental seismicity

This seismic sequence, which began on August 24^{th,} 2016, is enclosed in an area of the Apennines bounded by the 2009 L'Aquila sequence to the south and the 1997 Umbria-Marche sequence to the north. The area of Norcia (near the epicenter of the mainshock 6.5 M_W) was affected by a seismic sequence in 1979, which is not shown in the figure because it occurred before 1985.

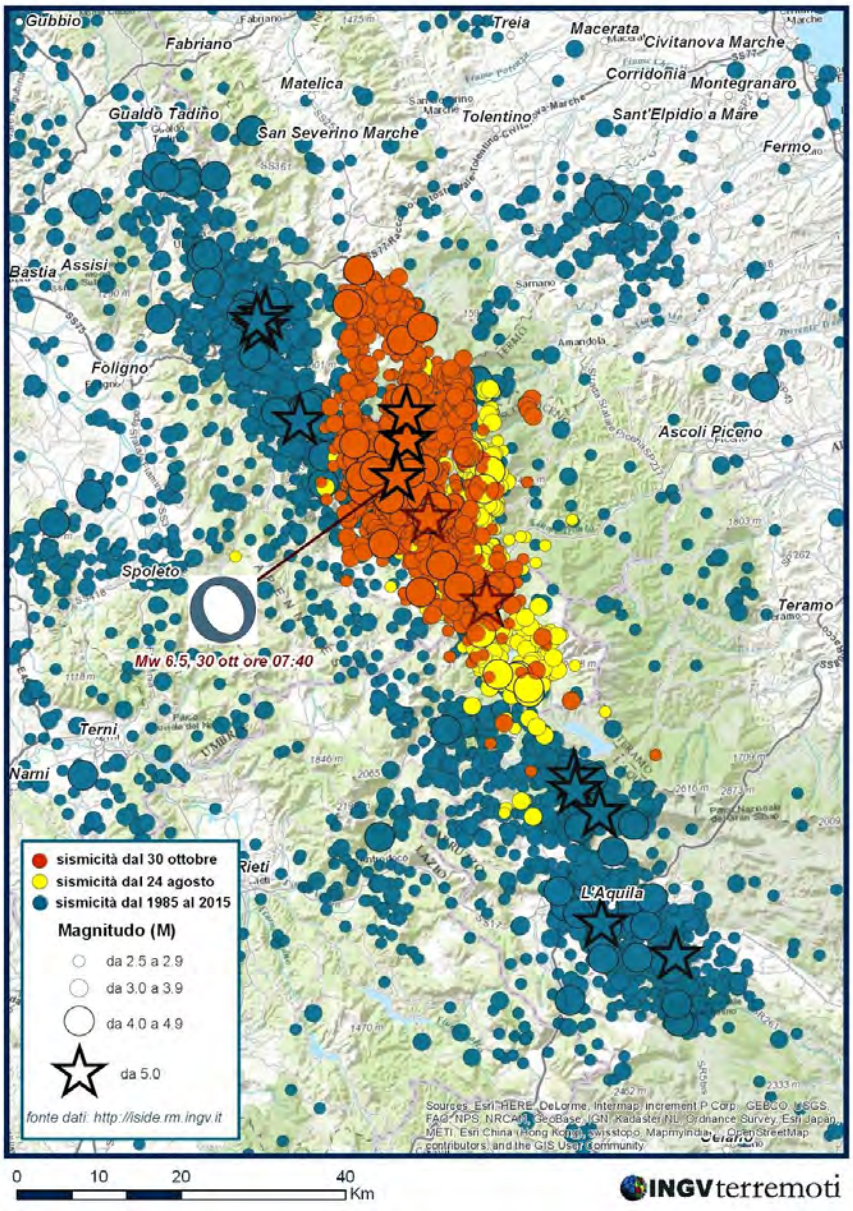

Figure 1.2.1 - Instrumental seismicity in the region since 1985. The different colors of the epicenters indicate different periods; blu epicenters 1985-2016 (July), yellow epicenters 24 August-25 October 2016, red 26 October 2016 3 November. Stars are events above magnitude 5.0.

1.3 Active faults

The area struck by the earthquake sequence is characterised by active fault systems already described in the geological literature published since the 90s of the past century.

In particular, the Apennine sector between Campotosto (south) and Colfiorito (north) presents normal fault systems trending NW-SE to NNW-SSE, with surface expression longer 20-30 km, made of minor fault sections 5-10 km long. The fault systems and the related fault sections are supposed to represent the superficial expression of seismogenic sources potentially responsible for earthquakes with M ranging between 5.5 and 7.0.
Apart from the case of Colfiorito (see below), evidence of recent activity has been related to the displacement of deposits and landforms attributed to Upper Pleistocene-Holocene, in many cases corroborated by paleoseismological investigations.
Based on the available literature, active fault systems can be defined as follows:

1) Mt. Vettore fault system, between the northern slope of the Tronto valley and the zone of Ussita, including sections along Mt. Vettore western slope, Mt. Argentella, Palazzo Borghese, Mt. Porche and Mt. Bove (Calamita and Pizzi, 1991; Coltorti and Farabollini, 1995; Cello et al., 1997; Pizzi et al., 2002; Galadini and Galli, 2003; Pizzi and Galadini, 2009). Seismicity occurred since August 24 2016 has been attributed to the activation of this fault. Considering the evidence of Holocene activity and the lack of associated historical earthquakes, the fault was considered as "silent", meaning that it may represent a seismic gap (Galadini and Galli, 2000). Moreover, surface faulting (see below) has been observed along the minor splay paleoseismologically trenched in 1999 by Galadini and Galli (2003).

2) Colfiorito fault system, characterised by three segments between the basins of Colfiorito (north) and the village of Mevale (south). This system is considered as the superficial expression of the seismogenic sources which caused the 1997 sequence (Cinti et al., 1999; Pantosti et al., 1999; Cello et al., 2000; Calamita et al., 2000; Vittori et al., 2000; Messina et al., 2002; Chiaraluce et al., 2005; Barchi and Mirabella, 2009). The amount of Quaternary displacement has been estimated in a few hundred metres. However, it is due to activity mainly occurred during the Early Pleistocene, while the evidence of Late Quaternary tectonics at surface seems negligible (Messina et al., 2002). The current fault activity has been considered consistent with a seismogenic behaviour related to the origin of earthquakes with M not larger than 6 (Messina et al., 2002).

3) Norcia fault system, between the villages of Cittareale to the south and Preci to the north, made of four fault sections: three of them bordering basins characterised by Quaternary deposition (Norcia, Campi, Preci); one (Cittareale-Castel Santa Maria) without associated basin and displaying evidence of deep-seated gravitational slope deformations (Calamita and Pizzi, 1992; Calamita et al., 1982; 1995; 1999; 2000; Blumetti et al., 1990; Blumetti, 1995; Brozzetti and Lavecchia, 1994; Cello et al., 1998; Galadini and Galli, 2000; Pizzi and Scisciani, 2000; Pizzi et al., 2002; Galadini, 2006; Gori et al., 2007). The fault system is considered as the expression of the source which originated the Jan 14 1703 earthquake (e.g. Galadini and Galli, 2000; Boncio et al., 2004a). This conclusion is also supported by paleoseismological evidence (Galli et al., 2005).
Moreover, minor earthquakes have been associated to this fault system (i.e. 1328, 1730, 1859, 1979).
East of Norcia, the Cascia depression is related to a fault characterised by Quaternary activity (Calamita et al., 1982; Cello et al., 1997). Its relationship with the Norcia system is unclear. The 1599 earthquake has been associated to this fault (Galadini et al., 1999).

4) Laga fault system, between the Vomano and Tronto valleys. It borders two different geomorphic domains, *i.e.,* the Amatrice basin and the Campotosto plateau (Cacciuni et al., 1995; Galadini and Messina, 2001; Boncio et al., 2004b). Two different fault segments have been defined in the past, *i.e.,* Amatrice and Campotosto. Quaternary fault activity is negligible along the former, while it is striking along the latter, particularly during the Upper Pleistocene-Holocene (Galadini and Messina, 2001). Moreover, paleoseismological investigations were performed in 1998 along the Campotosto section, defining Holocene repeated fault motions (Galadini and Galli, 2003). This segmentation seems also consistent with the historical seismicity. Indeed, while the Amatrice fault section has been associated to the 1639 earthquake and contributed to cause the 2016 August 24 event, the Campotosto fault apparently did not activate in the past century. For this reason, similarly to Mt. Vettore, also in this case the hypothesis of a seismic gap has been invoked in the literature (Galadini and Galli, 2003).

5) Montereale fault system, located along the eastern border of the basin and the San Giovanni NW-SE trending hill. Quaternary activity has been indicated in some papers (Blumetti, 1995; Cacciuni et al., 1995; Galadini and Messina, 2001; Chiarini et al, 2014; Civico et al., 2016). The relationship between these faults and the other affecting the L'Aquila area to the south (e.g. Mt. Marine, Pettino), associated to the Feb 2 1703 earthquake, is unclear. Possibly, an earthquake of the 1703 sequence (Jan 16) was originated by these faults or by one of them (e.g. that bordering the basin close to Capitignano).

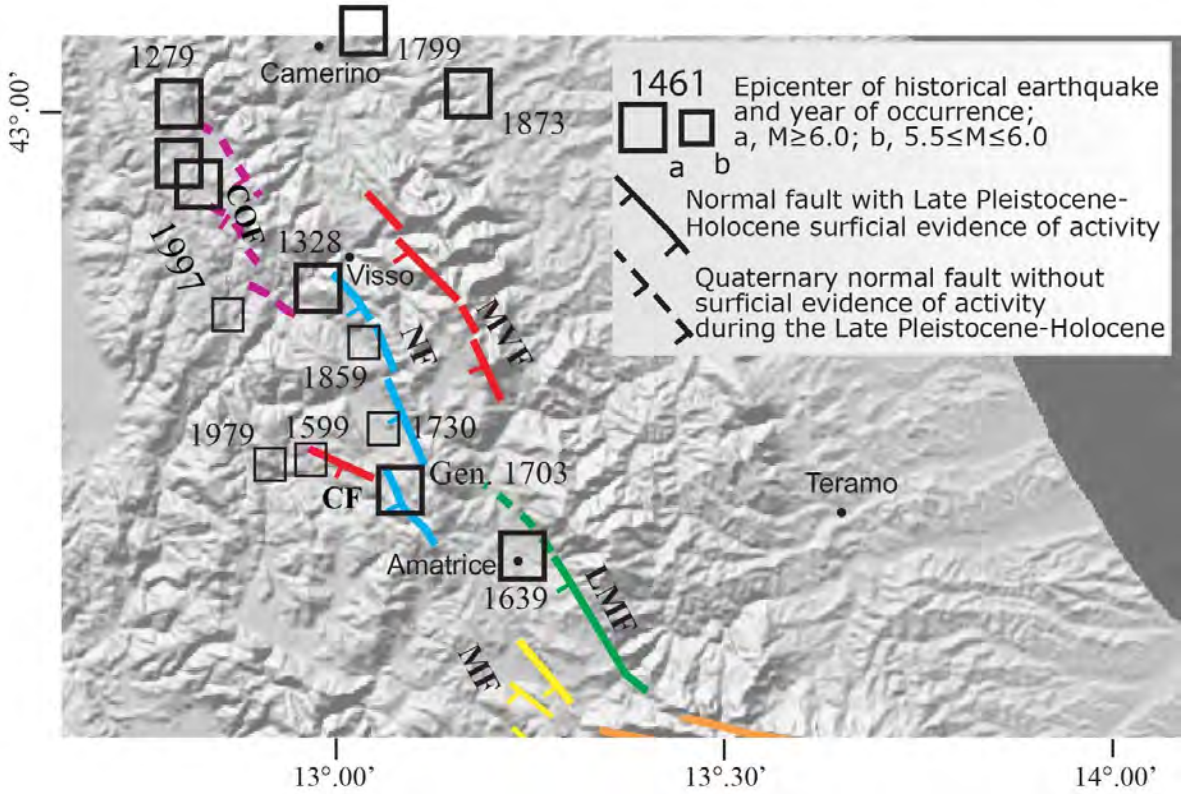

Figure 1.3.1 - Quaternary and/or active faults between the Montereale basin (south) and the Colfiorito area (north): COF, Colfiorito fault; MVF, Mt. Vettore fault; NF, Norcia fault; CF, Cascia fault; LMF, Laga Mts. fault; MF, faults of the Montereale basin.

1.4 Emergency seismic networks

Development of mobile seismic network until October 25th, 2016:
Following the strong earthquake of magnitude M_W 6.0 on August 24, 2016 at 01:36 UTC that struck the central Apennines [Gruppo di lavoro INGV sul terremoto di Amatrice, 2016; 2016b], SISMIKO (the coordination group of the emergency seismic network of INGV) prepared a plan for the deployment of a temporary seismic network to supplement the permanent stations already in the epicentral area. During the last week of August, SISMIKO installed 17 stations - 12 with 6 components (3C velocimeter and accelerometer). Since September, 13 stations are acquired in real time at the INGV center in Rome, all archived in EIDA http://www.orfeus-eu.org/data/eida/index.html and some included in the seismic surveillance system refined locations [more details: SISMIKO Working Group, 2016]. We added to these 17 stations other 2 temporary stations both transmitted in real time, from EMERSITO group (AM05 [EMERSITO working group, 2016]) and (T1299) from the National Seismic Network (RSN) group. Overall in late September, the temporary seismic network consisted of 19 stations (including 4 recording locally in standalone mode). The data collected from standalone stations have been converted into international format SEED and stored in EIDA. In local recording mode there is also a network of 20 stations of the British Geological Survey. The SISMIKO data integrates with data from the INGV National Seismic Network.

Development of temporary seismic network from October 27th to November 6th, 2016:
on the evening of October 26th two strong M_L 5.4 and M_L 5.9 events shook the area north of the sequence, at the border between Umbria-Marche near the municipalities of Castelsantangelo Sul Nera, Norcia and Arquata del Tronto. The area activated on October 26th is adjacent to the one active from August 24th, and extends the active area from Visso area towards the North for a length of about 10 km, up to Pieve Torina. For this reason SISMIKO decided to densify the seismic network to the North with the installation of three more temporary stations one of which (T1256) in real-time and included in the INGV seismic monitoring system. The other two (T1219 and T1220) were deployed in standalone mode. On October 30th, after the earthquake 6.5 M_W, SISMIKO prepared a further installation in the west area of the sequence, near Clitunno Campello in Perugia. The station is in real time and also T1220 was equipped with a UMTS router.

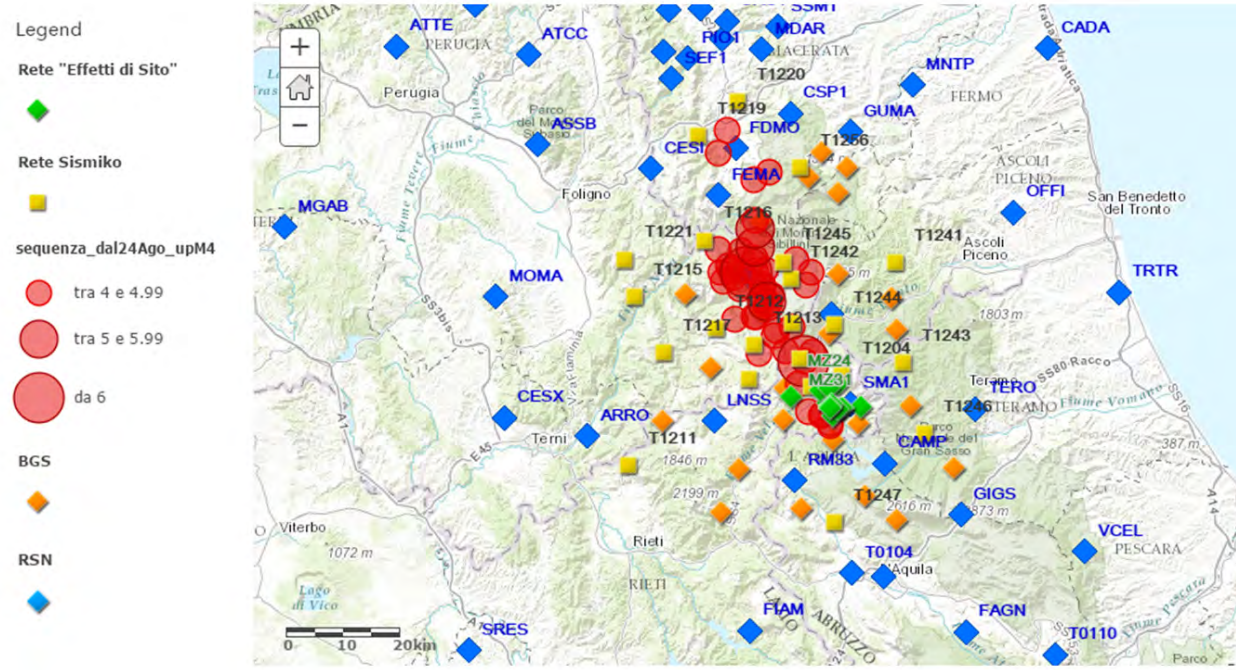

Figure 1.4.1 - Map of the seismic monitoring networks installed in the area affected by the earthquake sequence.

2. Mainshock

2.1 Focal mechanism

The focal mechanism of the earthquake is similar to those of previous earthquakes of the sequence, showing the extensional faults oriented NNW-SSE direction.
The non-negligible component of non-double couple (CLVD) could be related to a remarkable complexity of the geometry of the rupture.

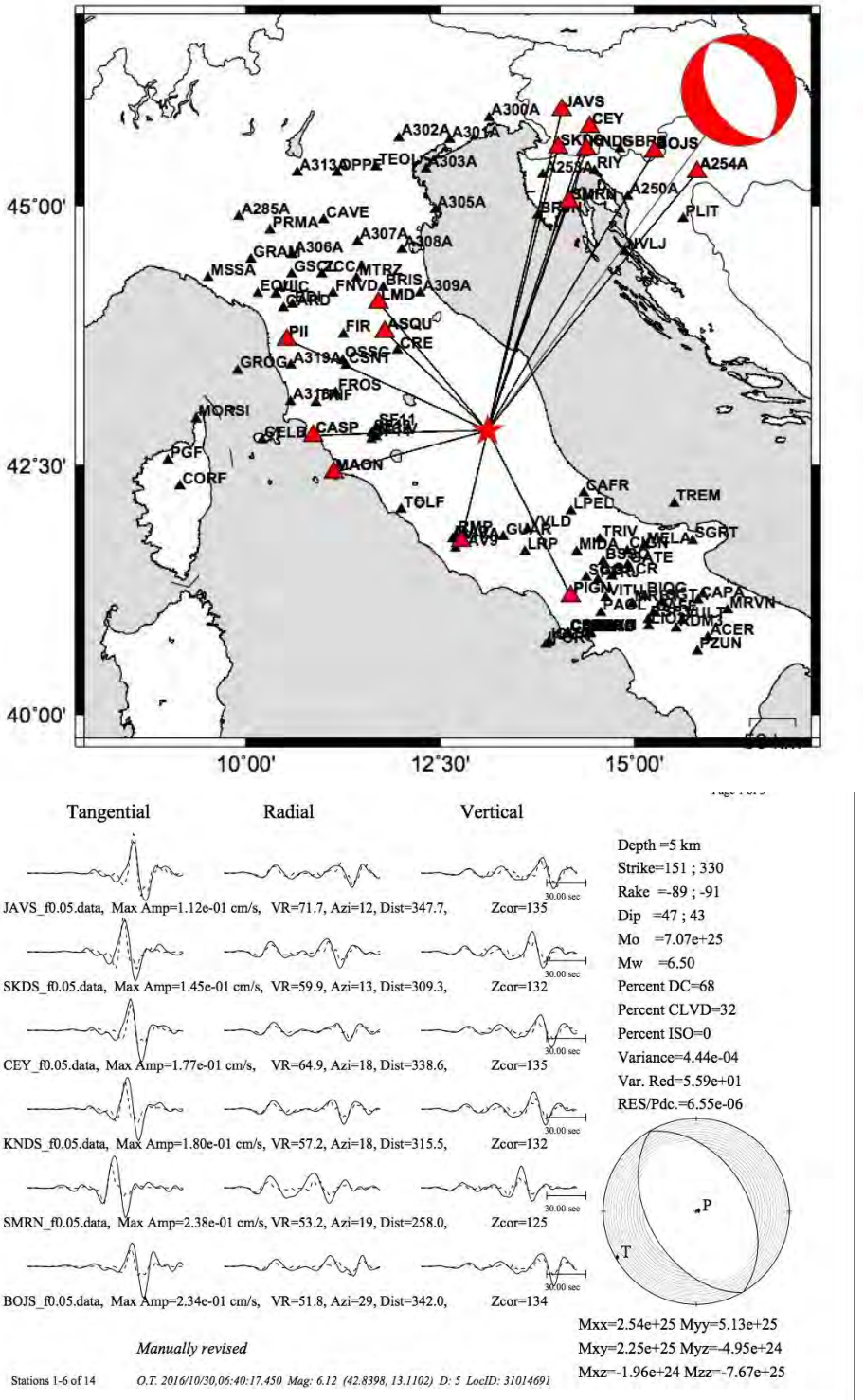

Figure 2.1.1 - TDMT of the mainshock *(http://cnt.rm.ingv.it/tdmt). On the same web page it is also possible to view solutions for events with smaller magnitudes. Other moment tensor solutions, for the same events evaluated with a different technique, are available in the Quick Regional CMT Catalogue (http://autorcmt.bo.ingv.it/quicks.html).*

2.2 Strong Motion Data

2.2.1 ISMD: real time analysis

Few hours from the 30 October 2016 M_W 6.5, mainshock origin time, all INGV accelerometric waveforms and related strong motion parameters were published at INGV strong motion database (ISMD, http://ismd.mi.ingv.it). The analysis considered both the permanent and the temporary (SISMIKO and EMERSITO) INGV networks installed in the first 250 km from the epicentre. On the web portal are available 195 strong motion waveforms recorded by 65 stations. Further 16 stations were not considered due to the low quality of the recorded data. In particular, considering epicentral distance < 50 km, 4 stations recorded peak ground acceleration (PGA) > 300 gal and further 6 stations PGA ranging from 100 gal to 300 gal. The maximum PGA was recorded at SISMIKO station T1201 (474 gal, NS component). For each considered station the web portal provides a site characterization based on geological, morphological and geophysical information. All data (accelerometric waveforms and related converted in velocity and displacement) and metadata are downloadable from the ISMD web site.

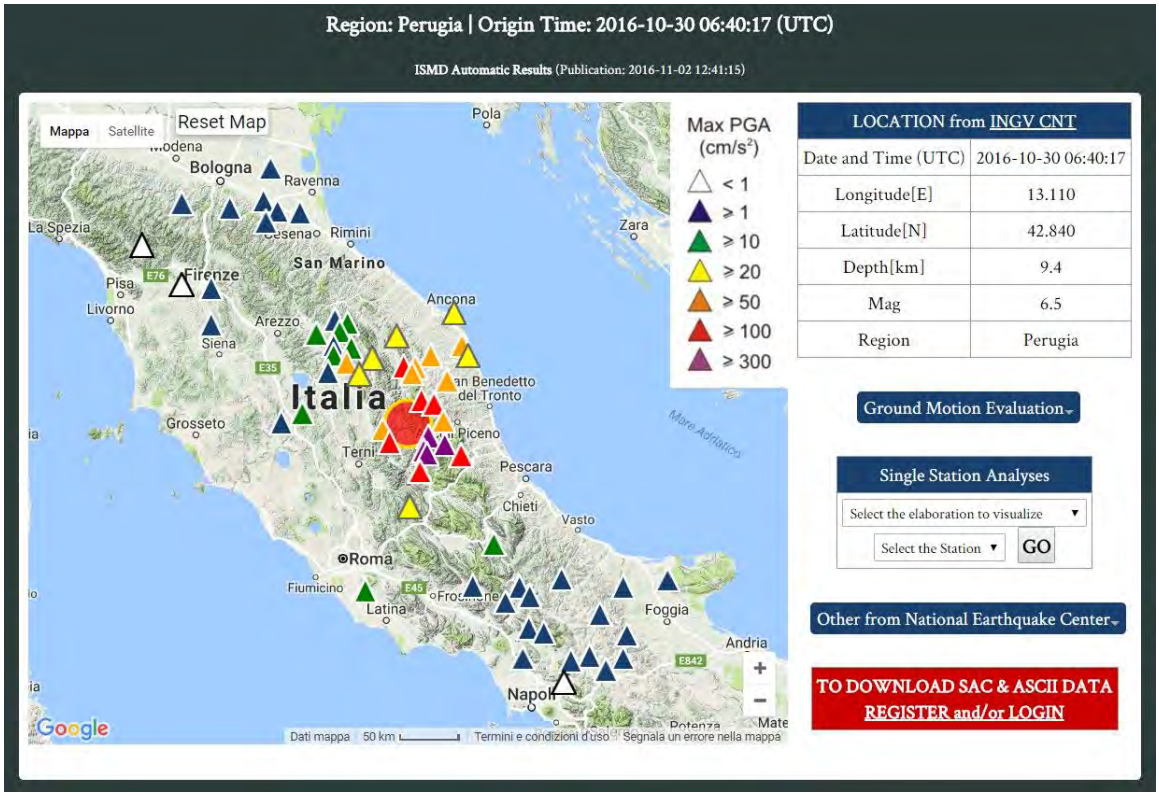

Figure 2.2.1 - Peak ground accelerations recorded by the INGV accelerometric stations during the 30 October (06:40:17), M_W 6.5, mainshock.

2.2.2 ESM: (Engineering Strong Motion database)

About 220 accelerometric signals have been manually processed using the procedure by Paolucci et al. (2011) and used to evaluate the peak ground motions, acceleration and displacement spectral ordinates. The manually processed records are available at the Engineering Strong-Motion database website (http://esm.mi.ingv.it). More than 12 stations have recorded accelerations larger than 300 gal within 30 km from the epicentre. The maximum acceleration has been observed at Accumuli (547 gal, Z component).

Figure 2.2.a shows the observed peak ground accelerations (maximum between horizontal components), whereas Figure 2.2.b shows the peak velocities.

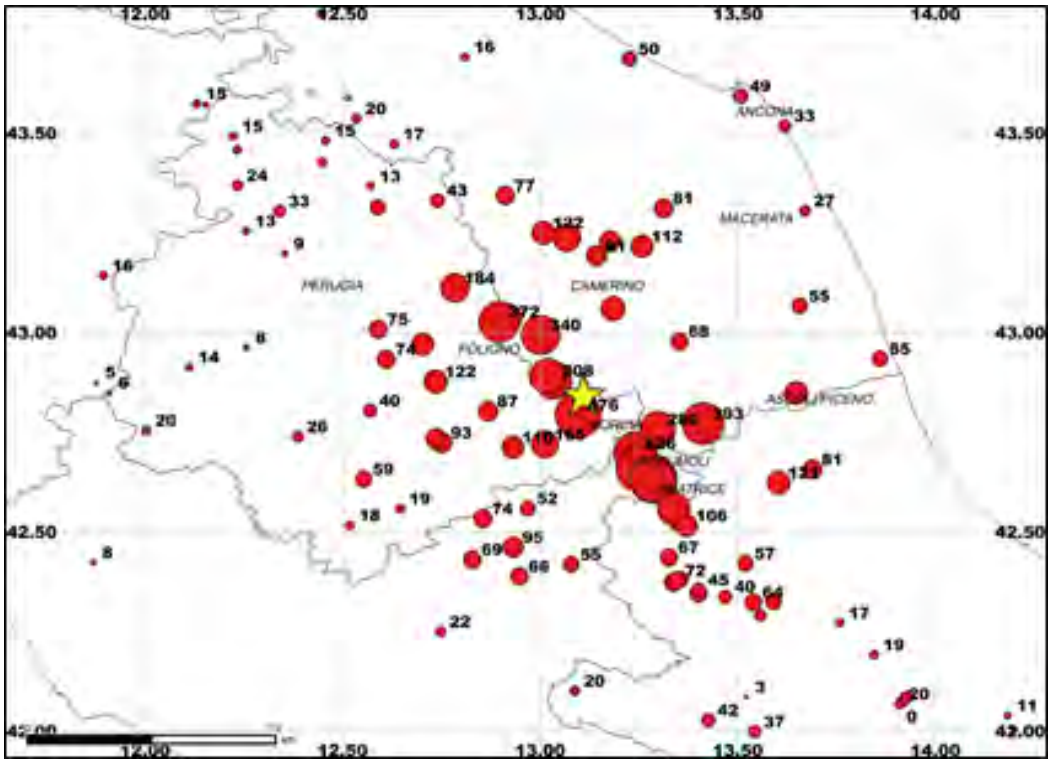

Figure 2.2a - Map of the observed peak ground accelerations (maximum between horizontal components).

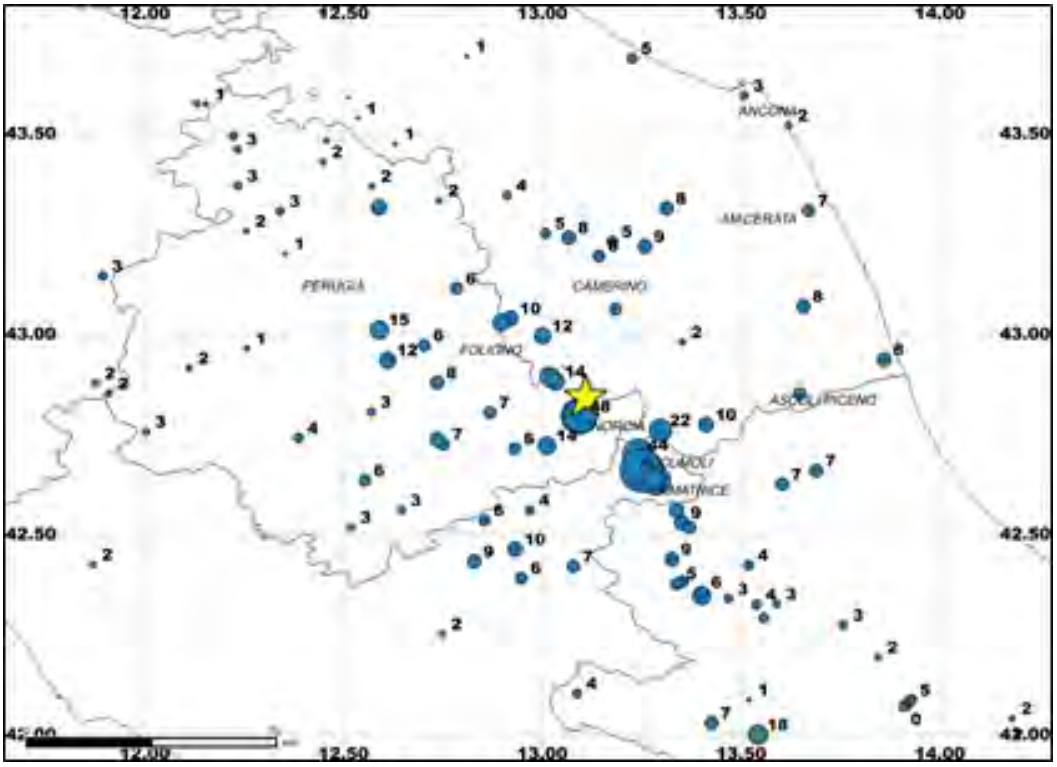

Figure 2.2b - Map of the observed peak ground velocities (maximum between horizontal components).

In order to analyze peak values and response spectra ordinates (acceleration and displacement), the processed data are compared to Italian (Bindi et al., 2011) and European (Akkar et al., 2014) Ground Motion Prediction Equations (GMPEs). The comparison is performed for the geometric mean of the horizontal components and distances are calculated from the surface projection of the preliminary fault geometry see strong motion source model in this report. Figure 2.2.c and 2.2.d show observations and GMPEs for peak ground acceleration and velocity, for the Ec8 (CEN 2003) soil categories (class A: Vs_{30} > 800 m/s; class B: Vs_{30} = 360 − 800 m/s; class C: Vs_{30} = 180 − 360 m/s; class D: Vs_{30} < 180 m/s; class E: 5 to 20 m of C- or D-type alluvium underlain by stiffer material with Vs_{30} > 800 m/s, where Vs_{30} is the average shear wave velocity in the uppermost 30 m). The observations agree with the prediction (GMPE median plus/minus one standard deviation) with few exceptions for soft soils (class EC8-C).

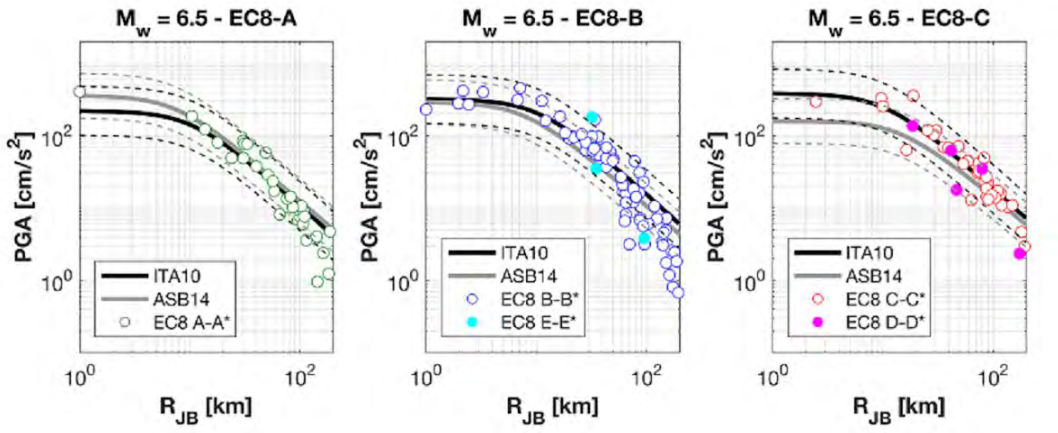

Figure 2.2c - Peak ground acceleration: comparison between GMPEs (Bindi et al., 2011, ITA10; Akkar et al., 2014, ASB14) and observations (geometric mean of the horizontal components).

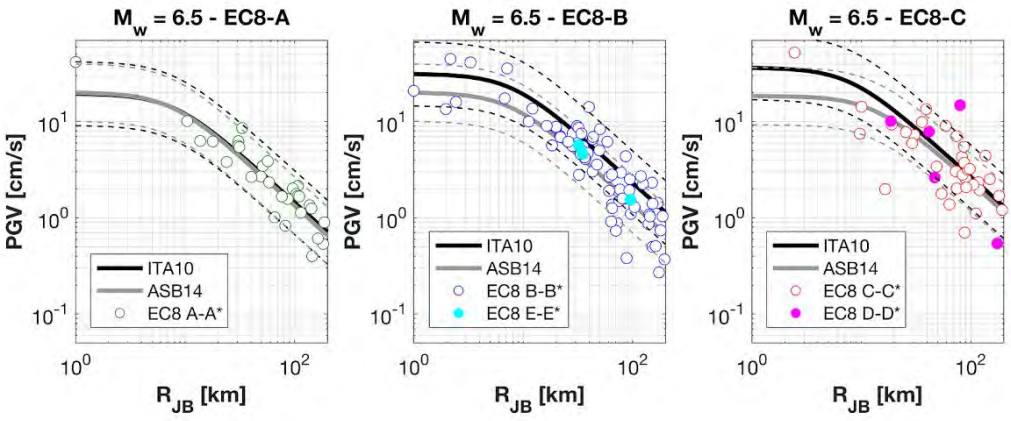

Figure 2.2d - Peak ground velocity: comparison between GMPEs (Bindi et al., 2011, ITA10; Akkar et al., 2014, ASB14) and observations (geometric mean of the horizontal components).

2.2.3 Strong motion variability and site effects

Following the M_w 6.0 Amatrice earthquake (24/08/2016), a temporary seismic network has been installed in the municipality of Amatrice to carry out preliminary investigations in the activities of seismic microzonation and geophysical, geomorphological, geological and geotechnical surveys (PCM Ordinance n. 394, 19/09/2016). The studies are performed in collaboration with other research institutes and universities participating to the Center for Seismic Microzonation (http://www.centromicrozonazionesismica.it/en/).

By the 30th of October, 14 stations were operating in the area, 7 of which installed in the Amatrice village and 2 chosen as bedrock reference sites (5-8 km away). Figure 2.2.1a shows the Z-component of the accelerations recorded for the M_w 6.5 event (30/10/2016), together with the vertical PGA; the maximum value was recorded at MZ12 station, near the church of St. Augustine, whereas the EW component recorded a PGA that exceeded 0.65 g. The waveforms in Figure 2.2.1a show a high variability and large PGA values inside the settlement. A

subsequent phase to S direct waves (about 6-7 s from the P first arrival) is also visible on all stations, including the two reference bedrock; this package has a frequency of 2-3 Hz and it is greatly amplified at MZ08 station (near the Ran AMT station) and near the historic center (MZ12 and MZ30). Spikes and spurious signals are probably linked to falling objects or building collapsing nearby.

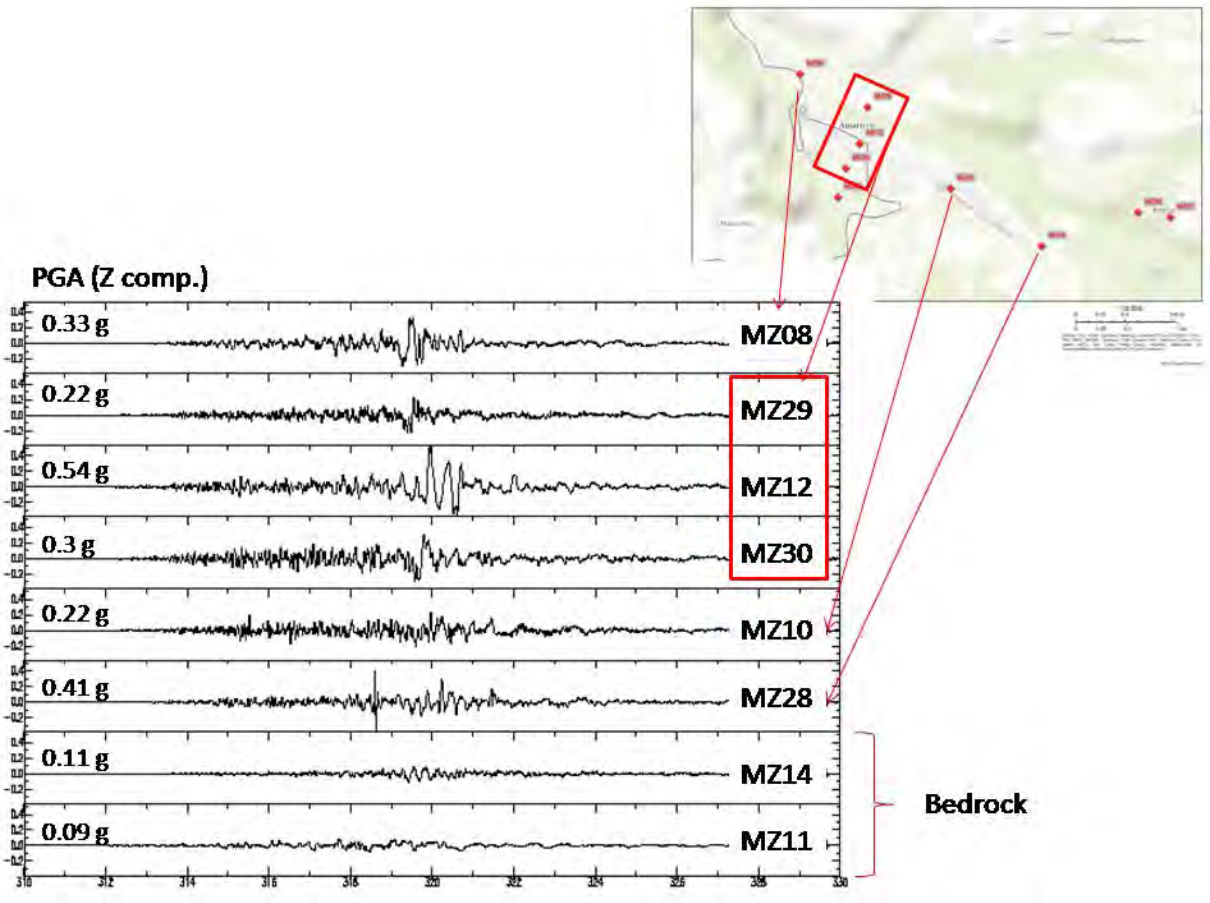

Figure 2.2.1a - Z component of the acceleration recorded in the village of Amatrice- San Cipriano during the M_w 6.5 earthquake (10/30/2016); for each station, the vertical PGA values are also indicated.

2.3 ShakeMap

The shake maps (ShakeMap) relative to the M6.5 earthquake of October 30 are shown in figures 2.3.1-2.3.2 in MCS intensity at local and regional scale, and PGA and PGV on a local scale, respectively (http://shakemap.rm.ingv.it/shake/8863681/products.html).

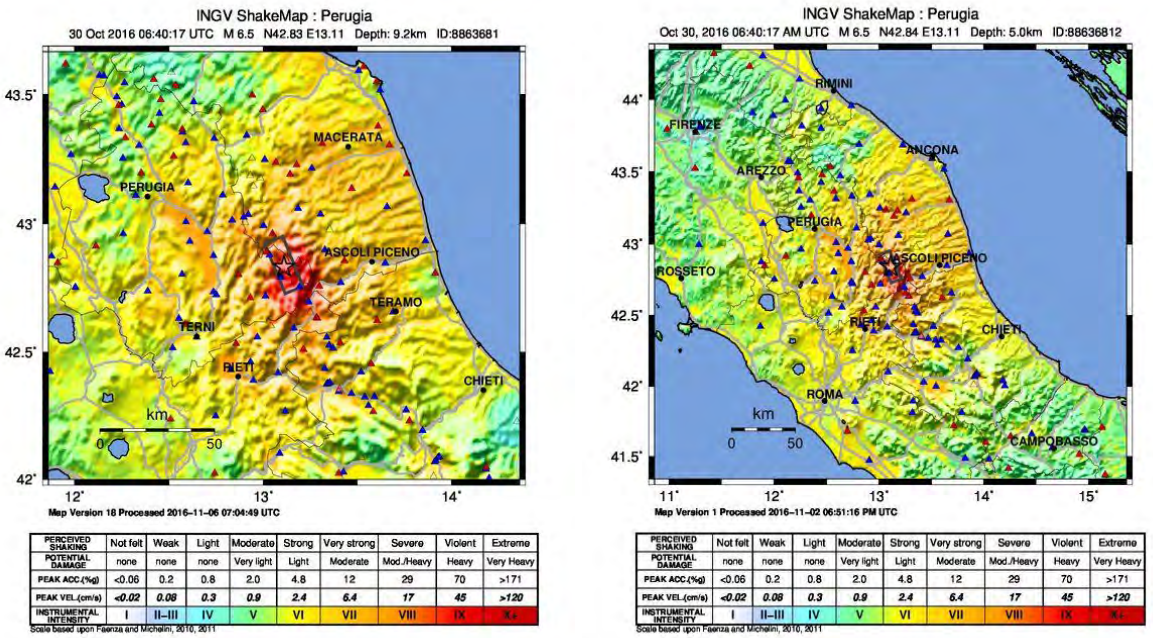

PERCEIVED SHAKING	Not felt	Weak	Light	Moderate	Strong	Very strong	Severe	Violent	Extreme
POTENTIAL DAMAGE	none	none	none	Very light	Light	Moderate	Mod./Heavy	Heavy	Very Heavy
PEAK ACC.(%g)	<0.06	0.2	0.8	2.0	4.8	12	29	70	>171
PEAK VEL.(cm/s)	*<0.02*	*0.08*	*0.3*	*0.9*	*2.4*	*6.4*	*17*	*45*	*>120*
INSTRUMENTAL INTENSITY	I	II–III	IV	V	VI	VII	VIII	IX	X+

PERCEIVED SHAKING	Not felt	Weak	Light	Moderate	Strong	Very strong	Severe	Violent	Extreme
POTENTIAL DAMAGE	none	none	none	Very light	Light	Moderate	Mod./Heavy	Heavy	Very Heavy
PEAK ACC.(%g)	<0.06	0.2	0.8	2.0	4.8	12	29	70	>171
PEAK VEL.(cm/s)	*<0.02*	*0.08*	*0.3*	*0.9*	*2.4*	*6.4*	*17*	*45*	*>120*
INSTRUMENTAL INTENSITY	I	II–III	IV	V	VI	VII	VIII	IX	X+

Figure 2.3.1 - Shakemaps expressed according to the MCS intensity scale of the 30/10/2016 M_w 6.5 earthquake. The two maps have been made using the same data set obtained primarily from the ESM DB (http://esm.mi.ingv.it). The map to the left is an enlargement of the right one. VI degree shaking affected an area of the Italian peninsula that goes roughly from Campobasso to the SE until Arezzo to NW, along the Apennine axis. The earthquake has been also well felt in the Po Valley. The stations of the national Seismic Network are indicated with red filled triangles whereas those of the national strong motion network (RAN) are shown with solid blue triangles.

Intensity shakemaps expressed using the MCS derived instrumental intensity scale of the 30/10/2016 M_w 6.5 earthquake. The two maps have been made with the same data set and the map of the left is an enlargement of the right one. It is evident that shaking until degree 6 affected an area of the Italian peninsula spanning from Campobasso to the SE to Arezzo toward NW, along the Apennine axis. The earthquake ground motion has been felt also as far as the Po valley.

The map shows PGV horizontal peaks reaching 77 cm/s at FCC and values above 40 cm/s recorded at the ACC and NRC stations.

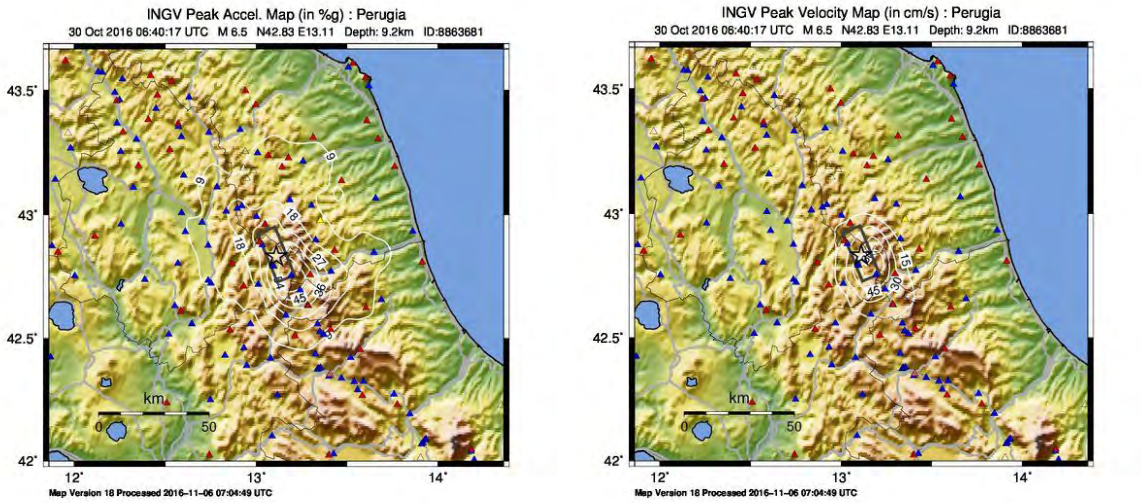

Figure 2.3.2 - Shakemaps determined using PGA (left) and PGV (right) values.

The maps have been all generated using the PGM (peak ground motion) parameters calculated from the data stored in the Engineering Strong Motion DB (http://esm.mi.ingv.it) and processed by experienced personnel. A procedure has been developed that checks and updates the shakemaps three times a day using the processed data entered in the ESM DB. The use of manually revised data allows for greater quality control of map-shaking produced.

2.4 Did you feel the earthquake?

The map in Figure 2.4a shows the distribution of effects in MCS (Mercalli Cancani Sieberg) scale over the territory of the earthquake of 30 October 2016, M=6.5.The map resulted by the elaboration of 12930 questionnaires filled by citizens, coming from 2680 municipalities, through the INGV dedicated site www.haisentitoilterremoto.it. Intensity was elaborated using the method described in Tosi et al., 2015. Purple star locate the instrumental epicenter, coloured dots refer to MCS intensity for each municipality. The size of the dot is proportional to the number of reports (see figure legend). Data were automatically and statistically tested and filtered (Sbarra et al., 2010; Tosi et al., 2015) for mistakes, but they were not verified individually. MCS intensities from VIII to XII degree are grouped together because, for a correct evaluation, such intensity data have to be verified by specialist technicians: a similar methodology is followed by the European-Mediterranean Seismological Centre (Musson, 2007). Moreover, considering that it is difficult to recognize the II MCS degree, because by definition it represents the effects perceived by only the 5% of population; we considered the I and II MCS degree as being in a single class.
The lack of information coming from epicentral zone, due to clear difficulties suffered by people in such areas, probably indicates an intensity of higher degree.

Generally intensity distribution shows a stronger attenuation with distance toward the Tyrrhenian side, in comparison with the Adriatic side. This difference confirms the analogous behavior of the 24 August 2016 M=6.0 event.

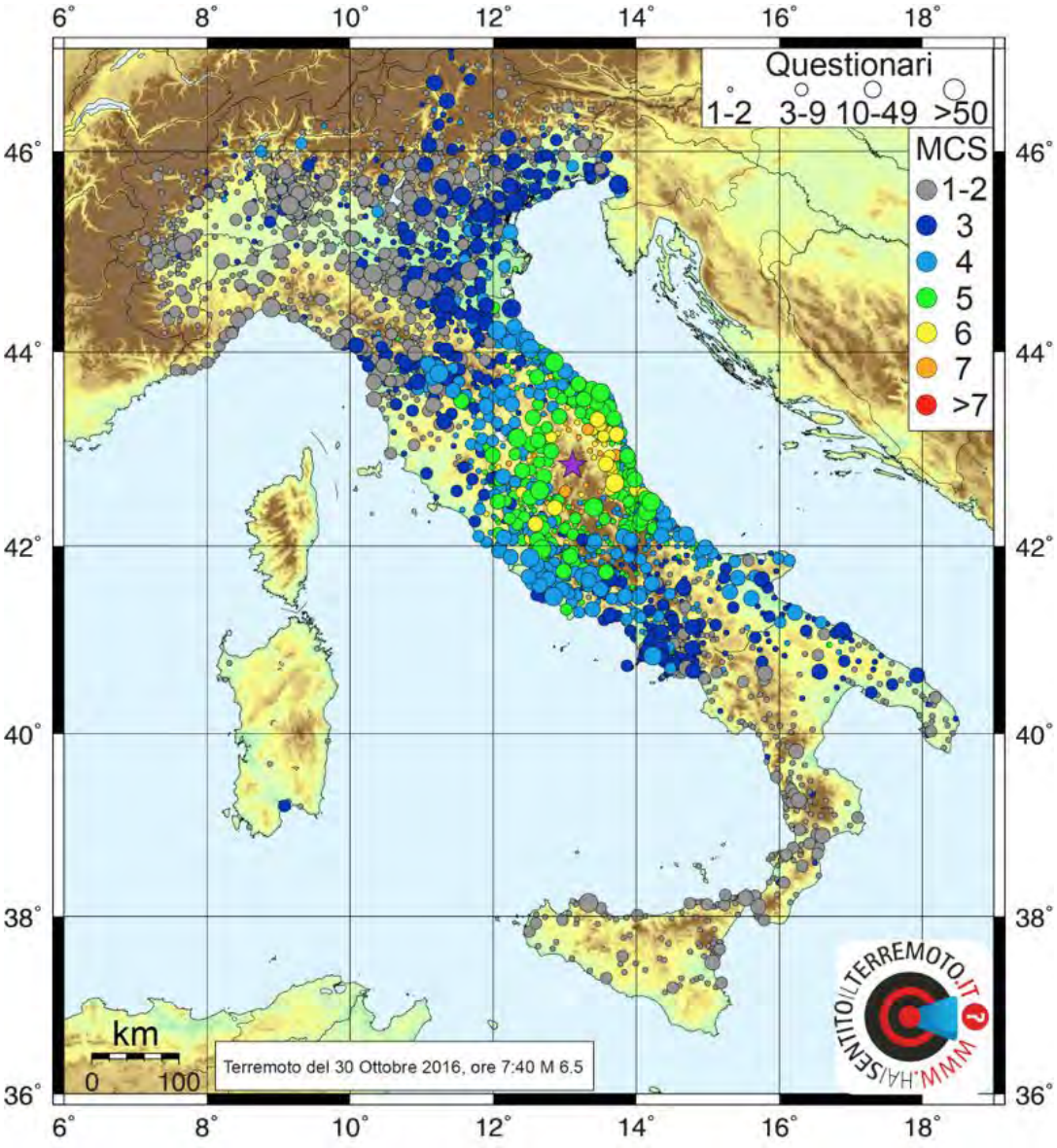

Figure 2.4a - Macroseismic intensity map of 30 October 2016 (7:40 local time) after the elaboration of 12930 macroseismic questionnaires filled by citizens, referred to 2680 municipalities, through www.haisentitoilterremoto.it web site.

The attenuation graph (Figure 2.4b) shows the municipality intensity versus epicentral distance (blue circles). On average V MCS degree was felt at 75 km from epicenter, IV MCS at 130 km and III MCS at 230 km. In Figure 2.4a, where macroseismic intensities are shown at regional scale, a certain degree of anisotropic attenuation is shown.

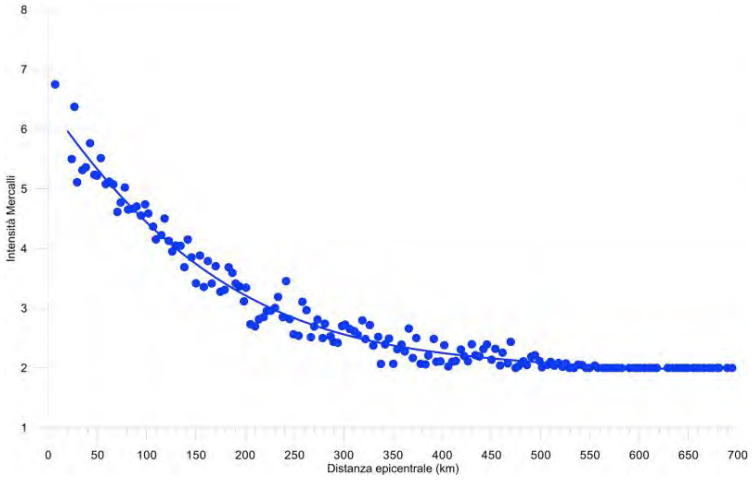

Figure 2.4b - Intensity attenuation graph versus epicentral distance of October 30 2016 earthquake (7:40 AM, local time).

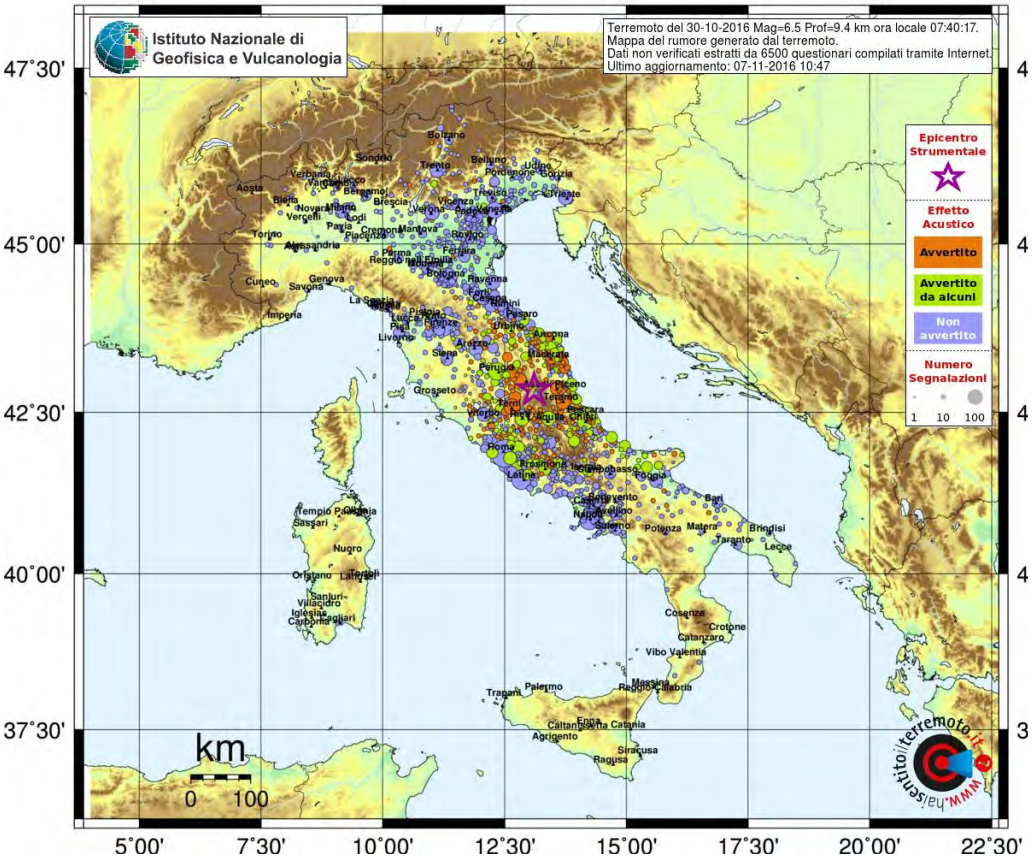

Figure 2.4c. - Geographical distribution of witnessed presence of seismic sound.

The map of the witnessed occurrence of an acoustic effect, also called seismic sound, (Figure 2.4c) is in agreement with macroseismic intensities, in particular with the higher perception toward Adriatic Sea side. On average the seismic sound was heard up to a distance of 150 km from epicenter.

2.5 Source models by Strong Motion data

We show here the preliminary kinematic source model on finite fault for the 30 October M_W 6.5 Norcia earthquake obtained by inverting the recordings of the 38 three-component digital accelerometers (RAN and INGV networks). The epicentral distances of the selected recording sites are less than ~45 km (green triangles on Figure 2.5-1). The recorded accelerograms were processed to remove the mean offset, band-pass filtered between 0.02 and 0.5 Hz using a low-pass and high-pass filters with two poles and two corners, and finally integrated in time to obtain ground velocities. We adopt the precalculated and stored Green's functions obtained using the CIA (Central Italian Apennines) velocity model [Herrmann et al., 2011].
We assume a fault plane striking 151° and dipping 47° to the SW, that is the fault geometry of one of the two nodal planes of TDMT focal mechanism.
The inversion code consists of a nonnegative, least squares inversion method with simultaneous smoothing and damping [Dreger and Kaverina, 2000]. The adopted fault dimension is 30 km long and 16 km width. The fault top reaches the surface. The best solutions that maximize the variance reduction are shown in Figure 2.5-1. This model has constant rise time of 2.1 seconds and rupture velocity of 2.5 km/s.
The most relevant feature of this model is a large and shallow slip patch, located at 4-6 km in depth, toward SE, having maximum values of 2.5 meters. Significative slip values (> 80 cm) are inferred also on the top of the fault in correspondence of surface offsets observed at Mount Bove - Mount Vettore. Total rupture duration of this model is 8 seconds. Even if the retrieved source model is able to capture the main features of the rupture history by producing a good fit with the data (VR=49%), the high value of the CLVD component retrieved by the MT solution, together with the complexity observed on near-fault recorded strong motion and the complexity of the DinSar interferograms, suggest us to keep on working on the cinematic inversions updating the presented model by introducing more complexities in the source geometry, e.g. the use of a fault system.

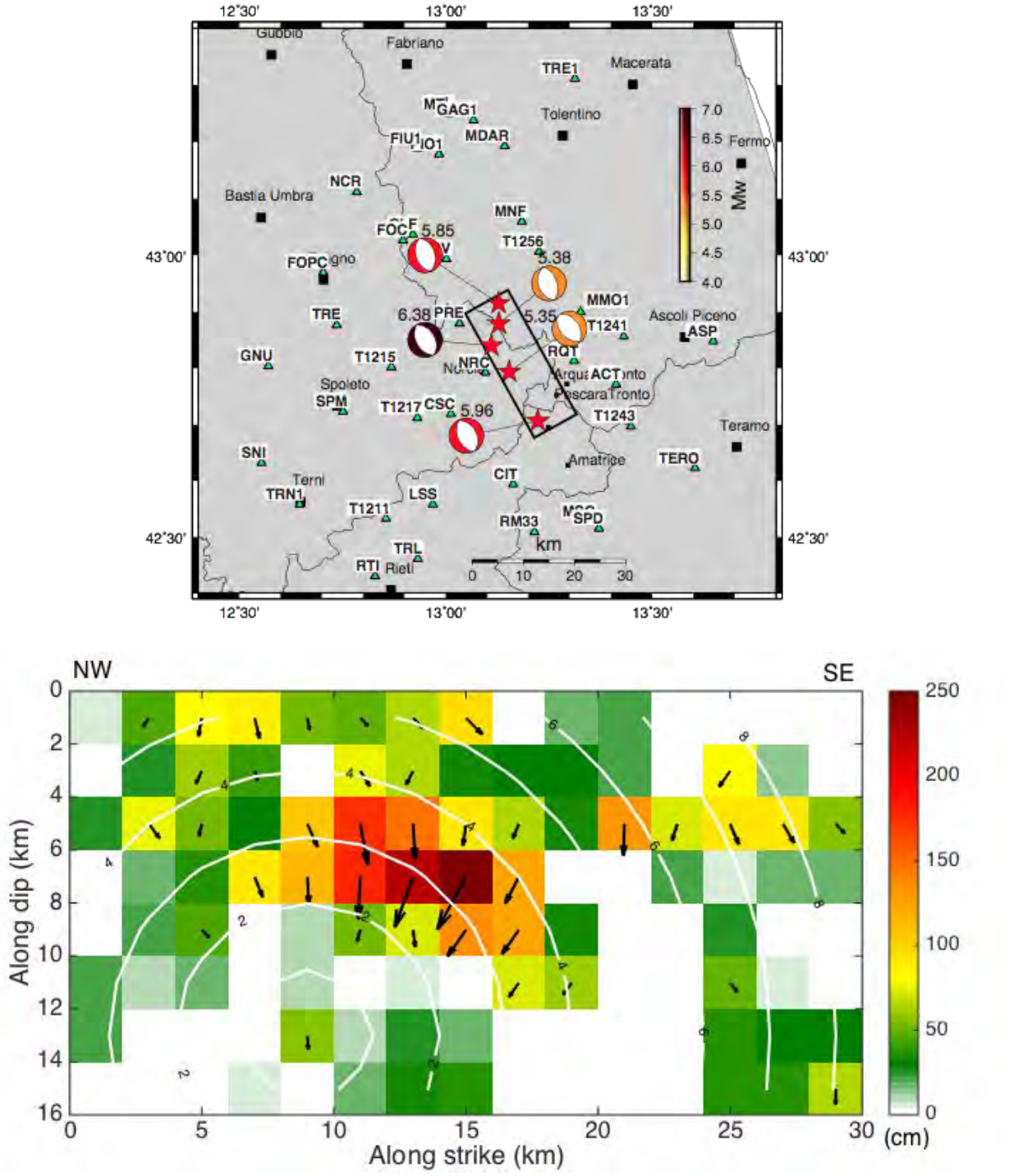

Figure 2.5.1 - a) Map of the accelerometers used during the inversion The black box indicates the surface projection of the fault plane dipping west; b) distribution of slip on the fault plane. The white lines indicate the time of rupture on the fault plane.

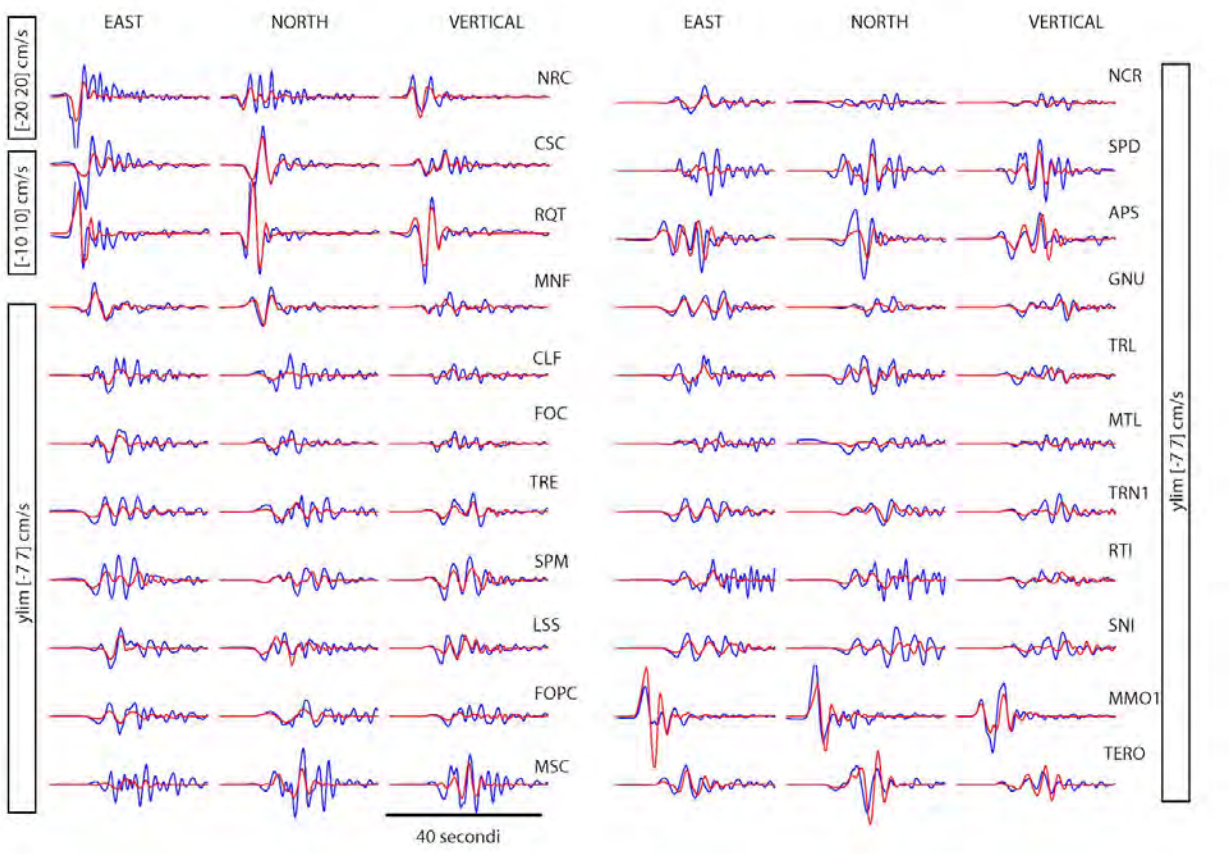

Figure 2.5.2 - Examples of fit to the data (in velocity): synthetic (red line) and the recorded data (blue line).

2.6 Propagation of seismic waves in a 3D velocity model

The preliminary kinematic finite fault model described in the previous paragraph has been adopted as input in the analysis of the seismic wave-field propagation. We use the software package SPECFEM3d_Cartesian (Peter et al., 2011), a spectral element code that take into account the major complexities as topography, 3D lateral variation of wave-speed, attenuation, anisotropy.

The wavespeed model adopted has been published by Di Stefano & Ciaccio 2014, a travel time tomography for the Italian region of Vp and Vs. The density is derived by an empirical function of Vp (Magnoni, 2014). The attenuation is included a simple model of Q as increasing linear function of Vs (Magnoni, 2014).

In figure 2.6a we report the material properties along the fault plane (as Vp and Vp/Vs ratio).

The simulation has been executed on 512 cores of INGV HPC cluster Auriga. As expected (Magnoni & Casarotti, 2016), the preliminary comparison show a decent agreement between data and synthetic seismograms, without exceeding the level of agreement show in the previous

paragraph, with the exception of the coda. We have analyzed with particular attention the preliminary pattern of coseismic displacement (3 minutes after dislocation), resulting from the simulation of the proposed kinematic model (Figure 2.6b).
The displacement exceed 2 meter threshold in the region of Mt. Bove - Mt. Vettore both for the vertical and the horizontal component. The preliminary deformation pattern well agrees with the first SAR images only in the eastern part of the epicentral area. In the western area, the geodetic data show a major complexity in the Norcia region, that is absent in our results. It is confirmed the need of a more complex kinematic model that involves a network of faults.

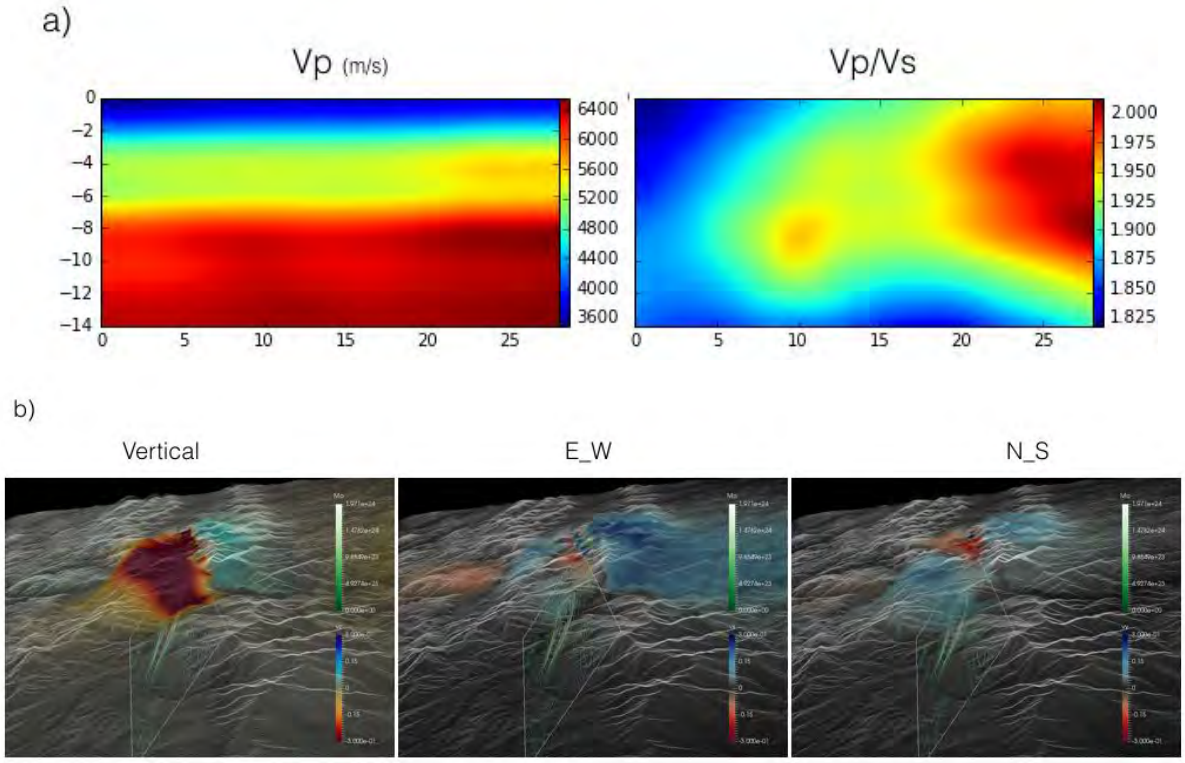

Figure 2.6 - a) values of Vp, Vs on the fault plane, b) seismic shift in the epicentral area, shows the vertical components, horizontal East-West and North-South. In Transparence the adopted fault plane that released the seismic moment.

2.7 Source models from GPS data

Following the August, 24 M_W 6.0 earthquake, INGV, in collaboration with the Ufficio Rischio Sismico e Vulcanico of the Dipartimento Protezione Civile (DPC) and the Servizio Geofisica of the Istituto Superiore per la Protezione e la Ricerca Ambientale (ISPRA), started a more detailed monitoring of ground deformation in the epicentral area using the Global Positioning System (GPS) technique (INGV Working group "GPS Geodesy", https://doi.org/10.5281/zenodo.61355).

In the following weeks, in fact, several GPS stations have been installed on benchmarks belonging to the INGV CaGeoNet network (Galvani et al., 2012) and of the Istituto Geografico Militare (IGM, www.igmi.org) network (Fig. 2.7.1). Moreover, a new INGV-RING continuous GPS station has been realized at Arquata del Tronto (ARQT). Following the October 26 events, we installed GPS instruments on a few IGM benchmarks that were already re-occupied during the 1997 Umbria-Marche seismic sequence (see Anzidei et al., 2008). Those stations recorded the co-seismic displacements of the M5.9 and M6.5 events of October 26 and 30. Not all the stations were operative simultaneously, because of electrical power problems and instrumentation movements over the different campaign benchmarks. Data from continuous and survey-mode GPS stations operating during the October 26 and 30 events have been downloaded in the following hours and days, and processed by the three INGV-CNT GPS data analysis centers, using three different analysis software (GAMIT/GLOBK, GIPSY and BERNESE), and later combined in a single, consensus, co-seismic solution, realized with the goal of minimizing the possible systematic errors present in the individual solutions (es., Devoti, 2012; Serpelloni et al., 2012). Figure 2.7.1 shows the measured co-seismic displacements for the October, 26 events and the distribution of the different GPS stations operating in the epicentral area from August, 24. Figure 2.7.2 shows the co-seismic displacements observed for the October, 30 event (note the different vector scales in the two figures). In both cases, the co-seismic displacements have been estimated starting from the position time-series, as the difference between the average position for the 17/10/2016-26/10/2016 interval and the the position at the 27/10/2016 for the October, 26 events, and the average position for the 27/10/2016-29/10/2016 interval and the position at the 30/10/2016 for the October, 30 event.

For the October, 26 events, the maximum horizontal co-seismic displacements have been observed at the stations FIAB (3.1 cm towards north-east) and CAMP (2.7 cm towards south-west), whereas SLLI has shown the largest vertical motion, with a subsidence of about 1.7 cm. As regard the October, 30 event, the largest horizontal co-seismic displacements have been measured at the stations VETT (Monte Vettore) and MSAN, with 38.3 cm toward north-east and 26 cm toward south-west, respectively. The largest vertical co-seismic displacements, instead, have been observed for the stations ARQT, RIFP and MSAN, with a subsidence of 44.6, 26.1 and 17.1 cm, respectively. The GPS station at Monte Vettore (VETT), instead, showed an uplift of 5.5. cm.

Figure 2.7.3 shows the results of a preliminary co-seismic slip model for the October, 30 event, obtained from the inversion of the displacements shown in Fig. 2.7.2. The inversion has been performed using a half-space elastic dislocation modeling approach, accounting for the topography of the area. In Fig. 2.7.3 the magenta rectangles show the coseismic faults obtained from non-linear inversion of the August, 24 and October, 26 events. In the slip inversion, instead, the fault plane for the M6.5 event has been fixed (length = 40 km, width = 18 km, dip= 45° e strike = 160°) and the slip distribution has been estimated on a discretized fault plane with patches of variable dimension (1x1 km down to 3.5 km of depth, and 3.5.x3.5 km for deeper patches) using the approach described in Cheloni et al. (2010). This slip model, which must be considered preliminary, shows a shallow slip concentration (with a maximum slip value of 2.5 m), corresponding to a M_w = 6.5.

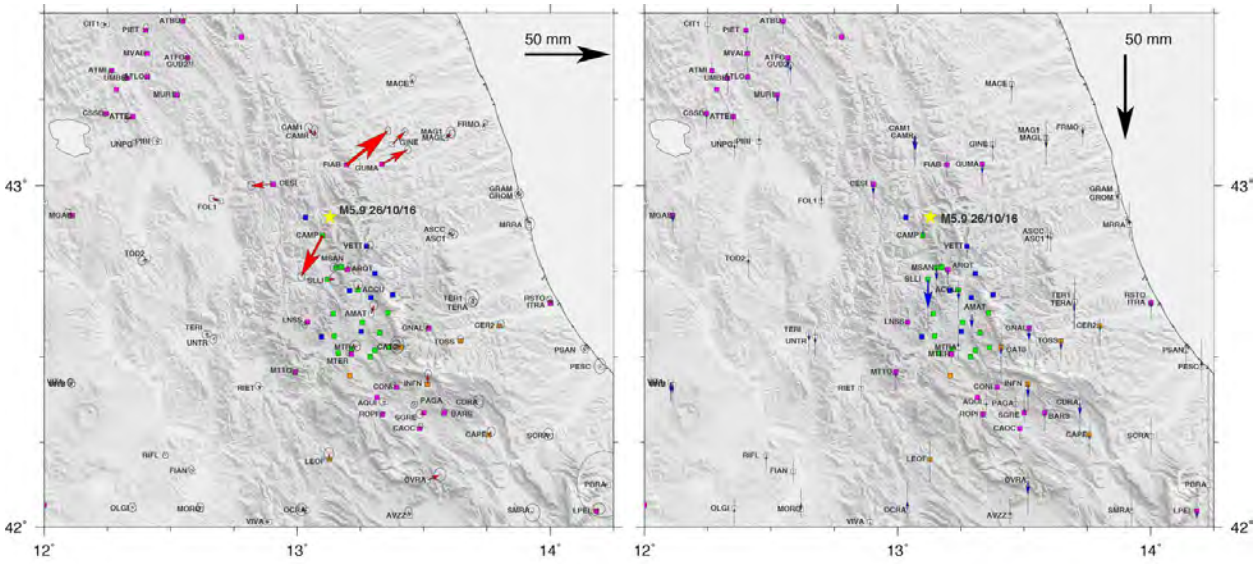

Figure 2.7.1 - Map of GPS horizontal (red arrows) and vertical (blue arrows) co-seismic displacements for the October, 26 events obtained from the combination of three independent geodetic solutions. The white squares show the position of continuous GPS stations, the magenta squares show the position of the INGV-RING (doi:10.13127/RING) continuous GPS stations. The orange squares show the continuous GPS stations managed by DPC and ISPRA. The green and blue squares show the benchmarks of the CaGeoNet and IGM networks re-occupied after August, 24.

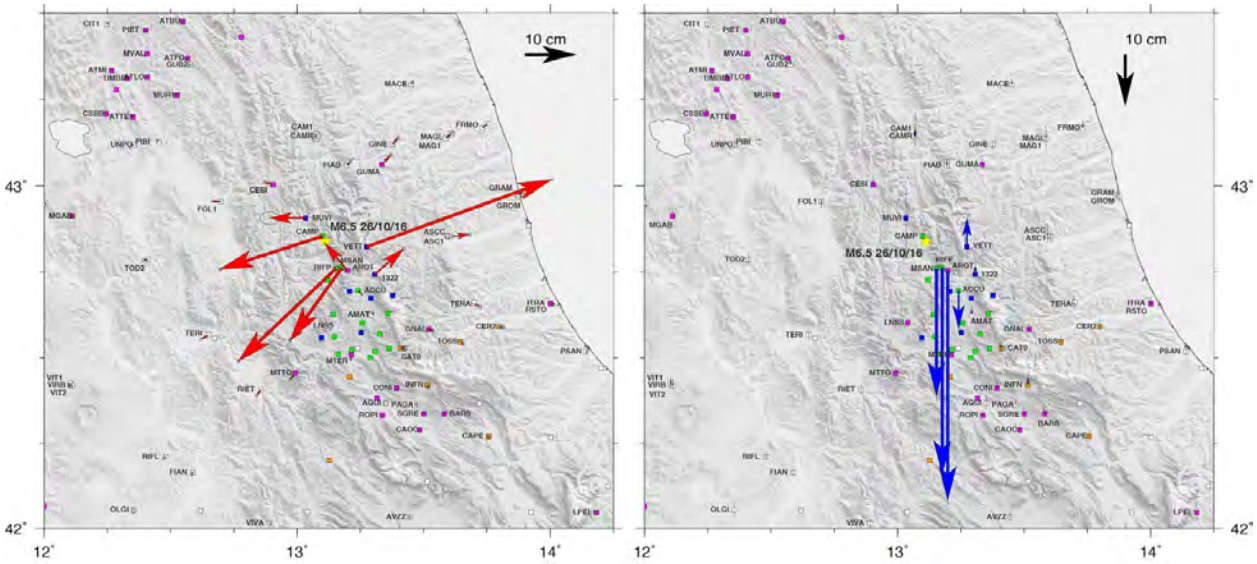

Figure 2.7.2 - Map of GPS horizontal (red arrows) and vertical (blue arrows) co-seismic displacements for the October, 30 event obtained from the combination of three independent geodetic solutions. The white squares show the position of continuous GPS stations, the magenta squares show the position of the INGV-RING (doi:10.13127/RING) continuous GPS stations. The orange squares show the continuous GPS stations managed by DPC and ISPRA. The green and blue squares show the benchmarks of the CaGeoNet and IGM networks re-occupied after August, 24.

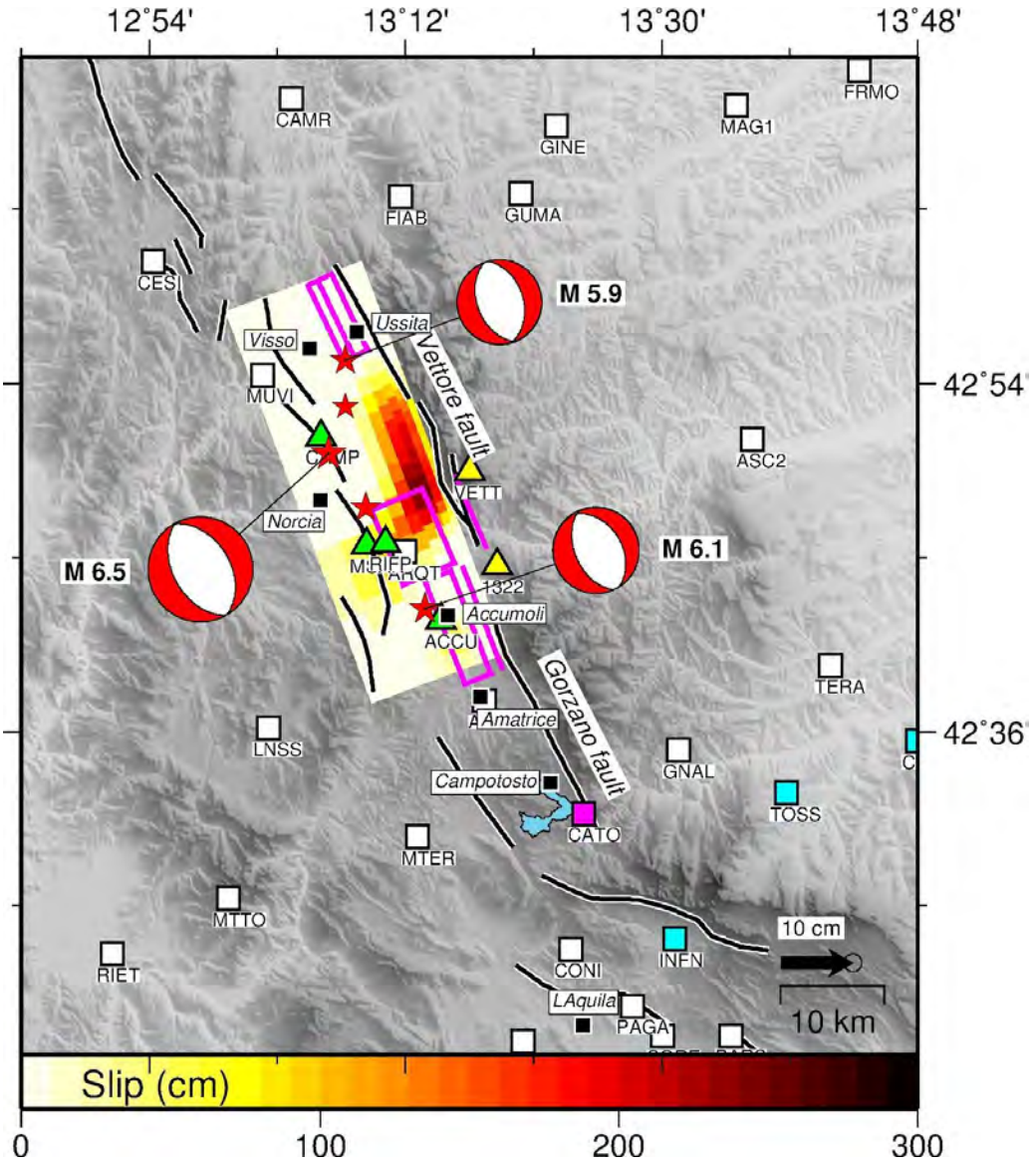

Figure 2.7.3 - Co-seismic slip model for the M_w 6.5, October, 30 event, obtained from the inversion of GPS displacements shown in Fig. 2.7.2. The magenta boxes show the co-seismic faults obtained from the non-linear inversion of GPS displacements for the August, 24 and October, 26 events.

2.8 InSAR measurements of ground deformation and source models

There are a series of co-seismic interferograms covering both the 26/10 and the 30/10 event. The following table lists the available image pairs and their characteristics.

ALOS-2	24 - 08 - 2016	11 - 11 - 2016	Ascending
Sentinel-1	27 - 10 - 2016	2 - 11 - 2016	Ascending
Sentinel-1	26 - 10 - 2016	1 - 11-12016	Descending

Table 2.8.1

In Figure 2.8.1 we show the descending Sentinel 1 interferogram (26/10 - 1/11), including both events. While the ground deformation in the far field is clear and with relatively low spatial deformation rates, from ~1 to 5 cm/km, in the internal area east of the epicenter, a very complex deformation zone extended N-S for ~30 by 10 km show much higher spatial gradients, up to ~30 cm/km. In this area the minimum LoS displacement of ~-80 cm is observed, near the Castelluccio plain. The broken pattern of several fringes on the western slope of the Mt. Vettore-Mt. Bove shows the presence of surface faulting, which is also observed in the field. Several other alignments of broken fringes indicating surface ruptures exist west of the main surface fault, some with similar orientation but many showing also different strike. One such pattern is cutting nearly in half the concentric fringe pattern north of Visso caused by the M 5.9 event of October 26. This small surface rupture occurred during the earthquake but cannot be attributed to direct surface faulting of the earthquake source since the projection of the latter is located more to the east.
The conclusion is that a large number of small surface fractures which can be observed in the field are likely due to a passive response of pre-existing faults to the dynamic and/or static effects caused by the main fault dislocation.
In Figure 2.8.2 we show the ascending Sentinel 1 interferogram 27/10 - 02/11, the first available today discriminating the 30/10 mainshock. The interferogram confirms the complex displacement pattern and the presence of features already highlighted above. In addition, it emphasizes a fringe pattern in the area around and westward of Norcia, composed of 9 concentric fringes probably due to the combination of displacements along vertical (uplift) and EW directions.

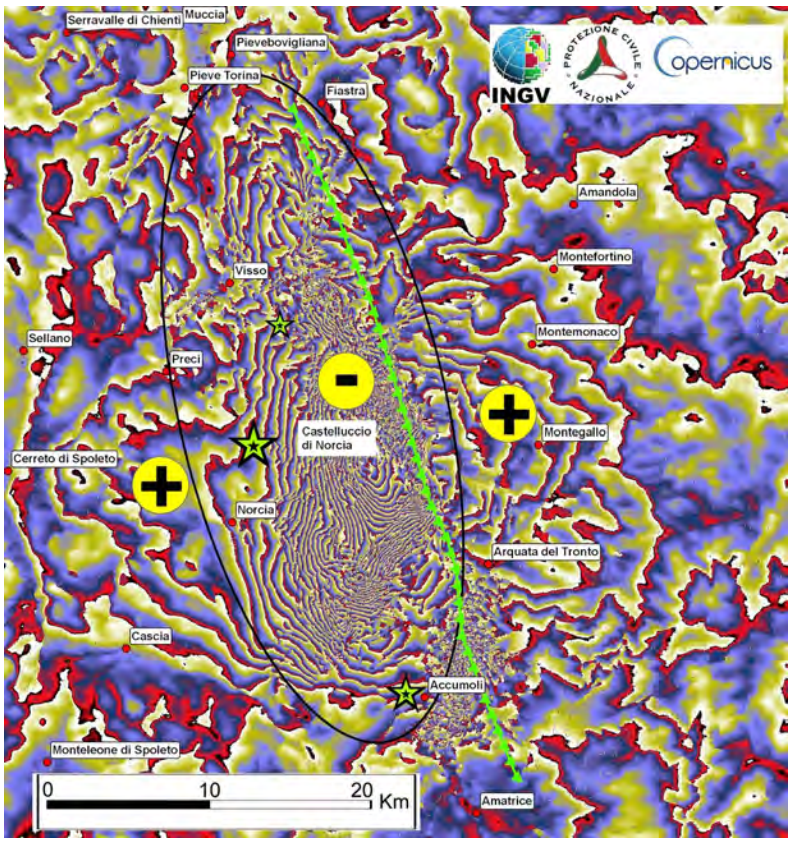

Figure 2.8.1 - Left, S1 descending interferogram (each fringe = 2.8 cm) showing the ground deformation of both the 26/10 and the 30/10 events (the green stars in the north). Yellow symbols show the uplifting and the lowering areas (along the LoS). The black ellipse outlines the complex deformation area, most of which is subsiding. Right, a detail showing some of the many ground fractures which can be identified in the interferogram. The long, easternmost line follows the location of the Mt.Vettore-Mt.Bove fault which has produced surface faulting.

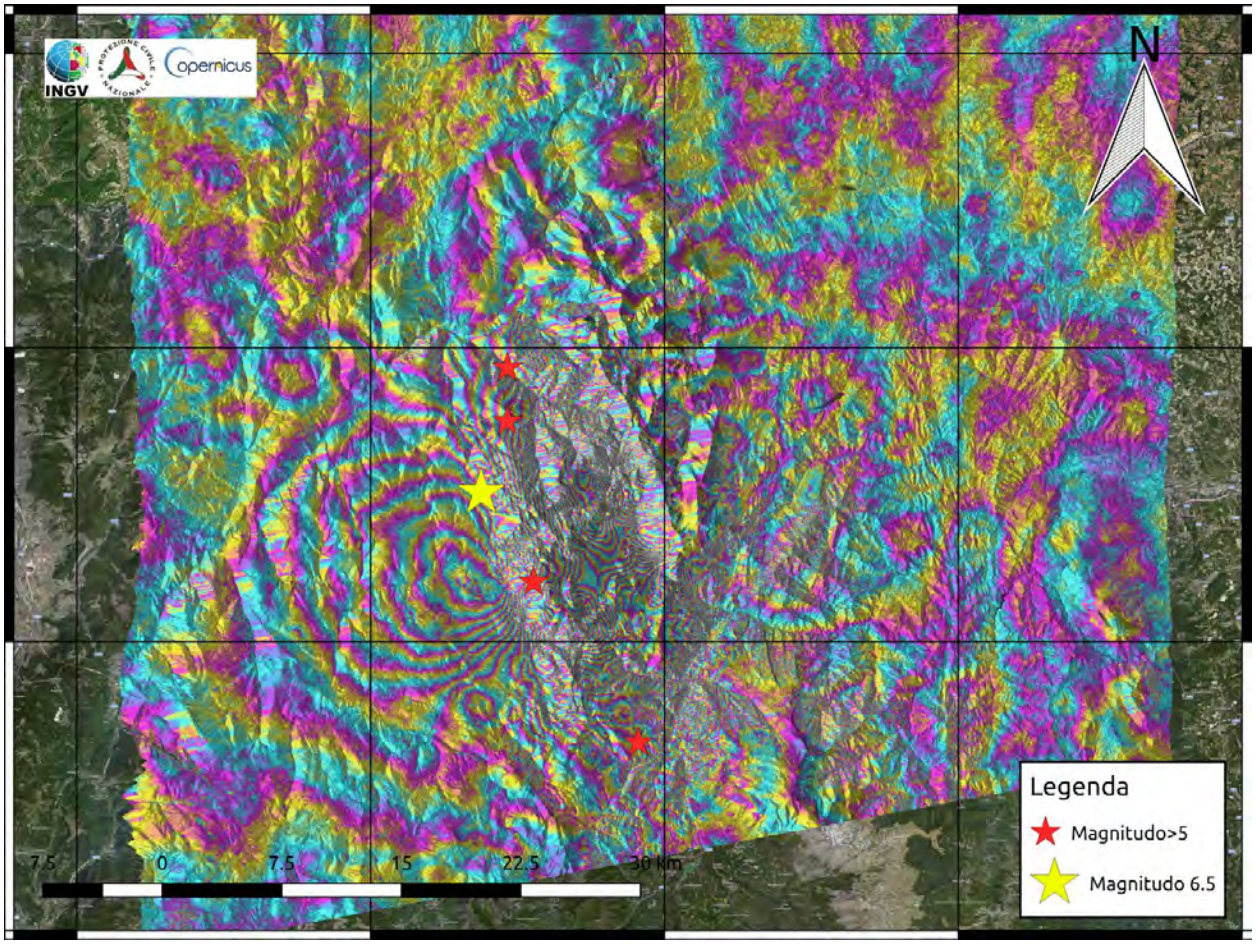

Figure 2.8.2 - S1 ascending interferogram (each fringe = 2.8 cm) showing the ground deformation of the 30/10 event (the yellow star). The complexity of the displacement pattern analysed in Figure 2.8.1 is confirmed. The interferogram emphasizes the concentric fringes in the area of Norcia and toward W. We count up to 9 fringes.

Due to the observed complexity, the unwrapped S1 interferograms (displacement maps) are affected by potentially large errors in the internal area. This effect is reduced for ALOS 2, although some unwrapping errors are still present in that result.
Indeed thanks to the longer wavelength (23.5 cm), the Japanese ALOS 2 is able to measure larger spatial displacement rates without exceeding the maximum detectable rate. The ALOS 2 pair, 24/08 - 02/11 (see Figure 2.8.3), contains the overall displacements due to the 26/10 and 30/10 earthquakes. Each fringe corresponds to an ~11.8 cm displacement in LoS. The coseismic pattern better highlights the local movements due to the above mentioned complexities and is able to point out local effects.

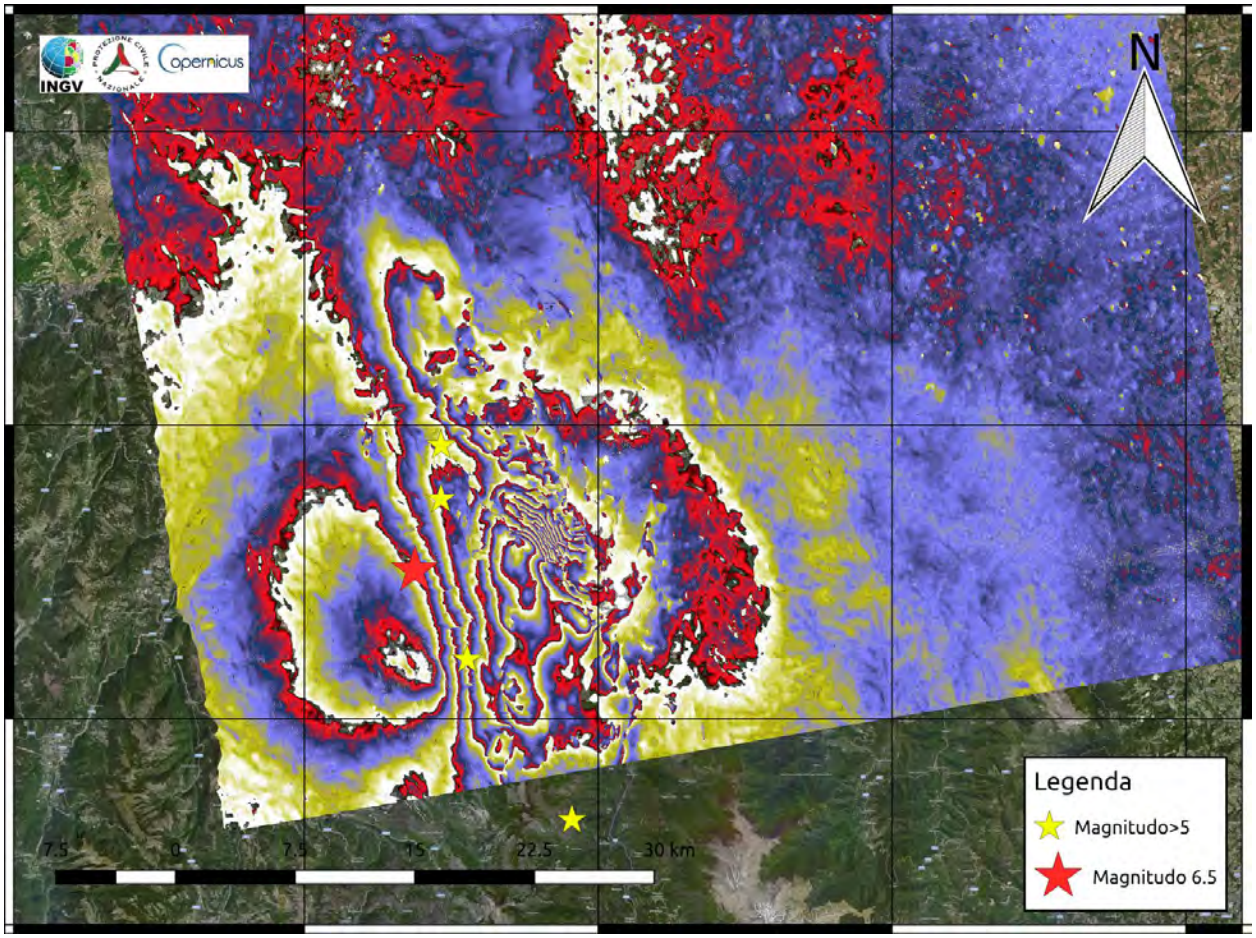

Figure 2.8.3 - ALOS 2 ascending interferogram (each fringe ~11.8 cm) showing the ground deformation of the 26/10 and 30/10 events (the red star). The interferogram emphasizes the features present in Sentinel 1 interferograms thanks to the exploitation of the longer wavelength. The concentric fringes in the area west of Norcia are confirmed.

We modeled the ALOS-2 ascending and Sentinel-1 descending acquisitions, to get a preliminary assessment of the October 30th source rupture. Though the model represents a first attempt to predict the complex pattern revealed by InSAR data, it clearly shows that most of the slip is distributed on a plane connecting the two ruptures of August 24th and October 26th (lighter in figure 2.8.4). The fault geometry has been constrained only with InSAR data and it shows a dipping angle slightly lower than the surrounding planes (about 30°). The slip distribution has a peak of about 2.8 m at a depth of about 3 km. It fills not only the gap between the two previous foreshocks, but also the local gap between the Mount Vettore shallow dip and the Vettore fault deep slip observed on August 24th.
A second source, apparently belonging to an antithetic structure and clearly visible in the interferograms, was modeled to explain a clear circular pattern in the southern part of the Castelluccio Plain. For this fault a normal mechanism was assumed.
The Moment Magnitude for this model is 6.5.

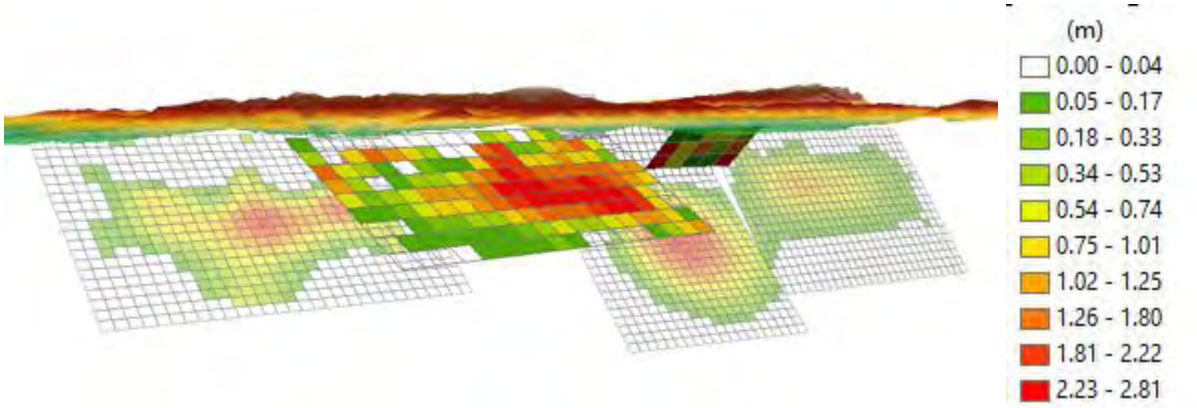

Figure 2.8.4 - Preliminary source model from InSAR data.

2.9 Surface Faulting

The October 30, 2016, M 6.5 earthquake rupture reached the ground producing an evident surface rupture along the Mt. Vettore – Mt. Bove Fault System (Figure 2.9.1). The day after this seismic event, an helicopter survey was performed, in collaboration with the Corpo Forestale dello Stato, allowing a quick recognition of the epicentral area and of the main coseismic deformation. Based on these data, a continuous surface rupture was mapped for a minimum length of 15 km between the Castelluccio di Norcia and Ussita towns (Figure 2.9.1). The coseismic rupture occurs along different fault splays of the tectonic system, e.g. along the sector of the MT. Vettore three main synthetic fault splays activated together with two antithetic tectonic structure. The amount of the deformation is quite important, reaching 2 meters, with a prevalent vertical component, along the main west dipping fault splays, both along bedrock faults and on unconsolidated deposits (Figure 2.9.2).

The activation of some antithetic structures (east dipping) was observed close to the main fault lineament (at hundred meters scale) as well as at kilometer scale of the entire basin. In fact, vertical displacements of few centimeters was recorded along the antithetic tectonic structure along the western slope of the Castelluccio plain, about 6-7 km far from the main fault.

Field and remote surveys, also in collaboration with national and international Research Institutions and Universities, are in progress and mainly focused on a detailed record of 1) total extension of the October 30 coseismic surface rupture, 2) its geometric characteristics and the dislocation amount, 3) the coseismic deformation distribution along the activated fault system.

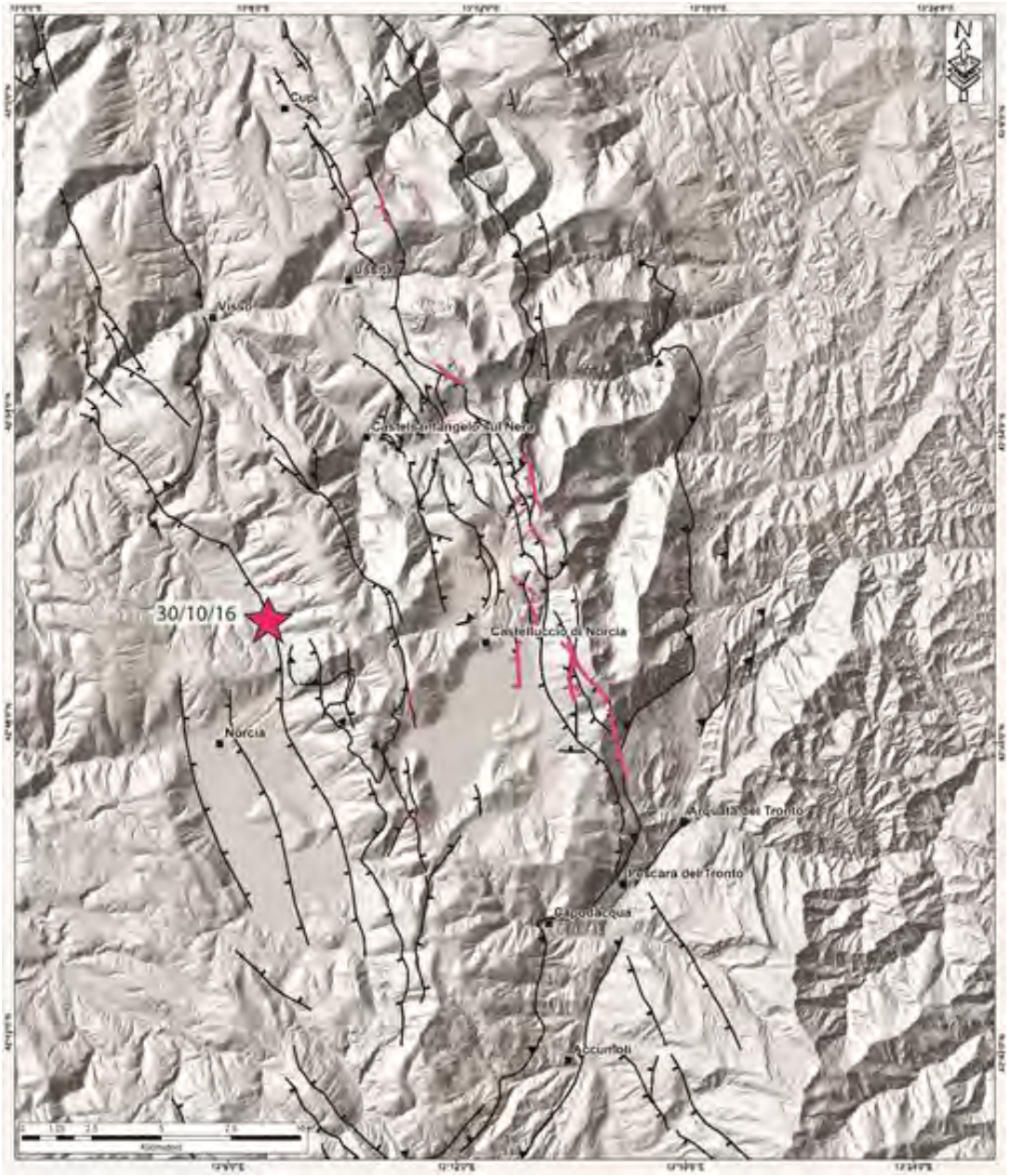

Figure 2.9.1 - Surface rupture (purple line) related to the 30th October 2016, M_W 6.5 earthquake (star locates the epicenter). Main active faults (black line) known in the area of the seismic sequence are shown.

A

B

C

D

Figure 2.9.2 - Pictures of the 30th October 2016 coseismic rupture. From above: A) free face on bedrock fault plane; B) ruptures along two fault splays along the western slope of the Mt. Vettore; C) fault scarp along the fault splay affecting the Castelluccio di Norcia plain, in the back the view of the western slope of the Mt. Vettore; D) scarp in unconsolidated deposits in the Mt. Bove sector.

The October 30, 2016, surface earthquake rupture partially overprints the August 24 mainshock surface deformation in the Castelluccio di Norcia sector, along the western slope of Cima del Redentore and Vettoretto peaks (Figure 2.9.3). In this sector, the amount of the coseismic deformation should be evaluated taking into account both the surface faulting events. Northward, between Ussita and Cupi towns, it is possible to observe a partial superimposition of the October 30, 2016, surface earthquake rupture with those related to the October 26 mainshock.

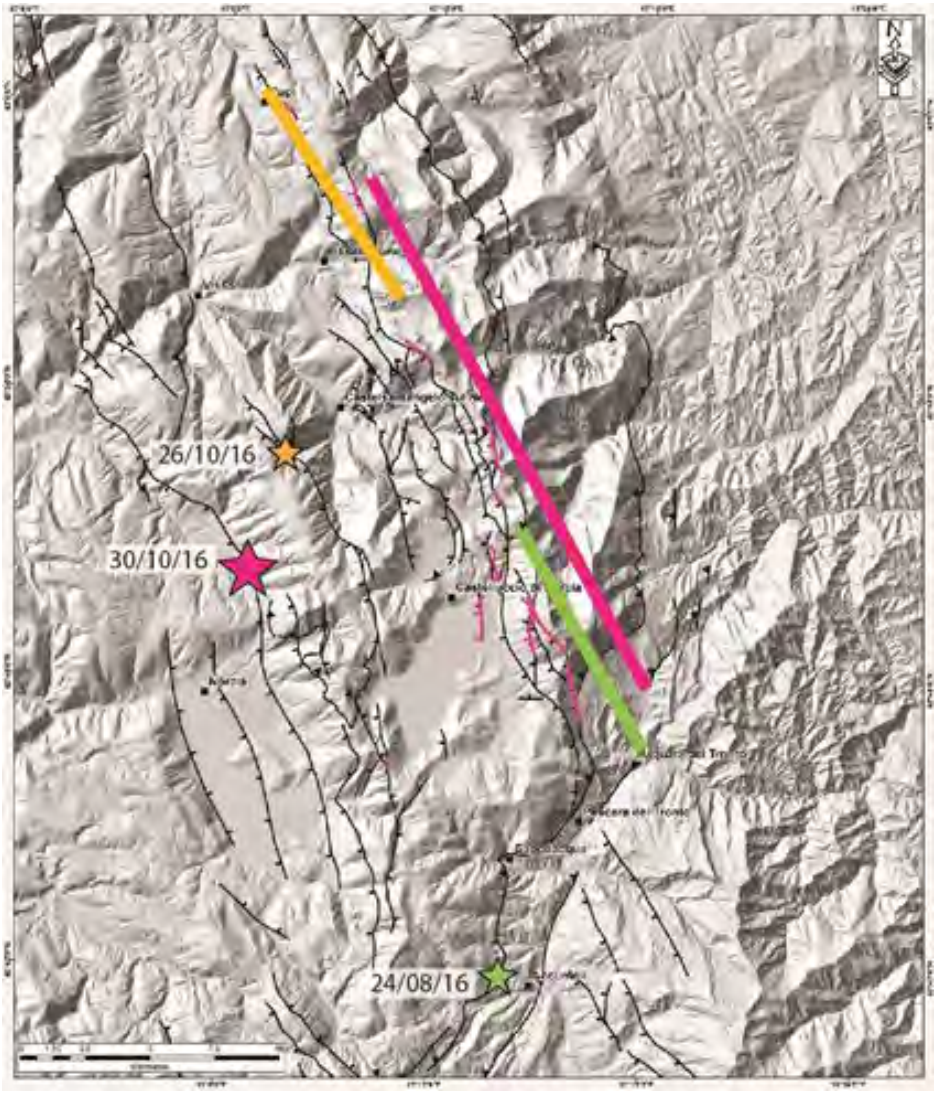

Figure 2.9.3 - Coloured bands indicate the sectors of the fault system along which coseismic ruptures occurred associated to the three main seismic events (24th August in green, 26th October in orange, 30th October in purple). Stars locate the epicenters of the three mainshocks (24th August M_W 6.0, 26th October M 5.9, 30th October M_W 6.5).

3. Seismic sequence

3.1 Space-temporal pattern of the sequence

The seismic sequence began on August 24th and immediately activated segment of the fault system about 40 km long, the portion north of the epicenter of the Amatrice earthquake was more active than the rest of the fault system. On October 26 a magnitude 5.9 event activated a northernmost segment further 15 km long. this portion of the fault system is still very productive today. With the very strong shock of 30 October 30th also the southern portion of the fault system throughout almost its whole length has been reactivated and is producing aftershocks.

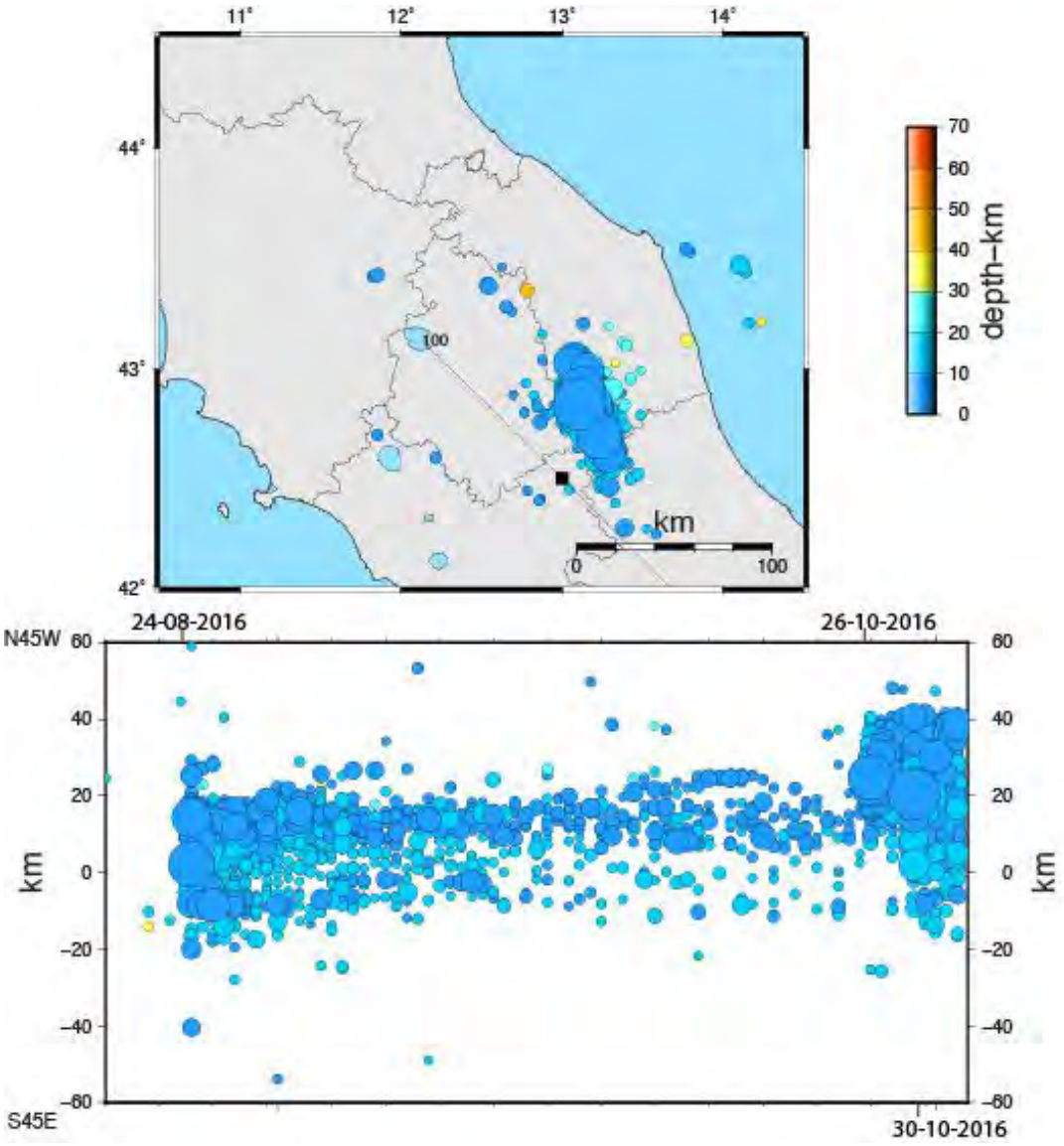

Figure 3.1.1 - Spatio-temporal pattern of the earthquake sequence of 2016.

3.2 The fault system imaged by earthquakes distribution; refined locations

We re-located the seismic sequence by inverting P- and S- arrival times, picked by the seismologists on duty in the seismic monitoring room of the INGV, promptly released thanks to standard web-services giving direct access to the real time database [Pintore et al., 2016].

We analyzed the events occurred in the period ranging from 2016/08/24 to 2016/11/04, recorded by the National Seismic Network (RSN, INGV) plus 12 additional stations installed soon after the mainshock by SISMIKO. We used the National Accelerometric Network (RAN, Civil Protection Department) data for the main shocks arrival times.

The velocity model used for the re-location is a gradient derived from the 1D velocity model of De Luca et al. [2009]. The earthquakes have been relocated with a non-linear inversion code [NonLinLoc; Lomax et al., 2009] because it provides a comprehensive description of the location uncertainties. To reduce systematic delays due to the use of a 1D velocity model we also used more than 300,000 P- and S- arrival-times to calculate (and then apply) stations corrections. Vp/Vs ratio was kept fixed to 1.85 (calculated for the sequence with the Wadati [1931] method) only for the Mw > 5.0 events. By applying a quality selection criterion (based on horizontal and vertical errors less than 1km and 2km, respectively; rms<0.5s and gap<180°), we ended up with a final catalogue composed by 18,403 events we show in map view and cross sections drawn perpendicularly (N65°E) to the fault segments. Selection criterion has not been applied for Mw>4.0 events. It is worth noting that the location quality will be improved with time by adding the information coming from the tens of stand-alone stations data. As a consequence, at this stage we prefer to avoid the description of the fault system and seismicity pattern details.

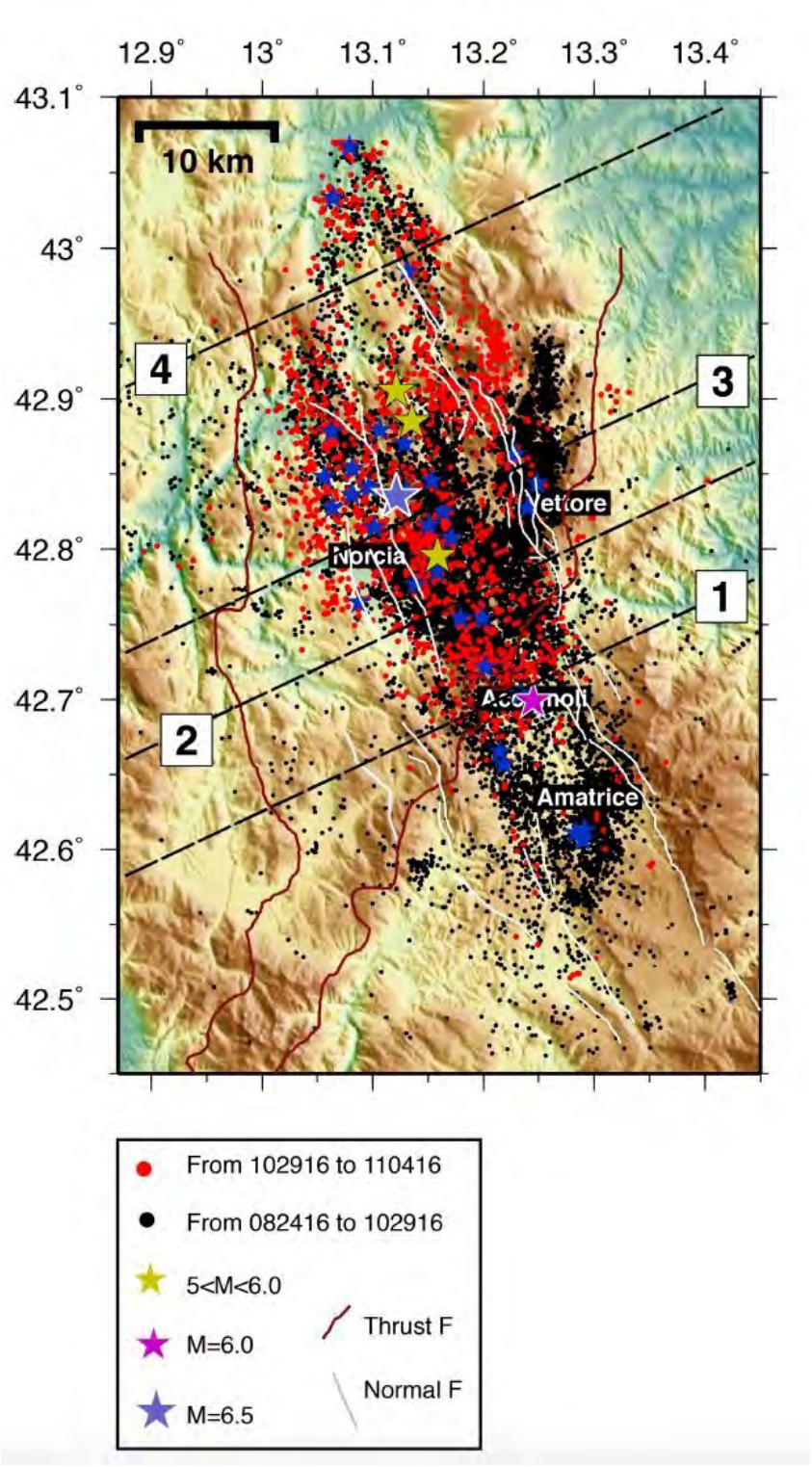

Figure 3.2.1 - MAP – Up to now the seismicity activated a 60 km long normal fault system. The black and red events are the ones occurred respectively before and after the M_w 6.5 mainshock. From the map view it is quite clear the role-played by the inherited compressional structure (e.g. Olevano-Antodoco Thrust) in driving the extensional deformation. The M_w 6.5 aftershocks are in fact all located on the NW-eastern portion of this tectonic line. Also the largest events occurred at the end of October are included in this portion of the system. The seismicity occurred after the M_w 6.5 event also insists along the basal layer with the occurrence of few M>4 events (e.g. sections 2 and 3).

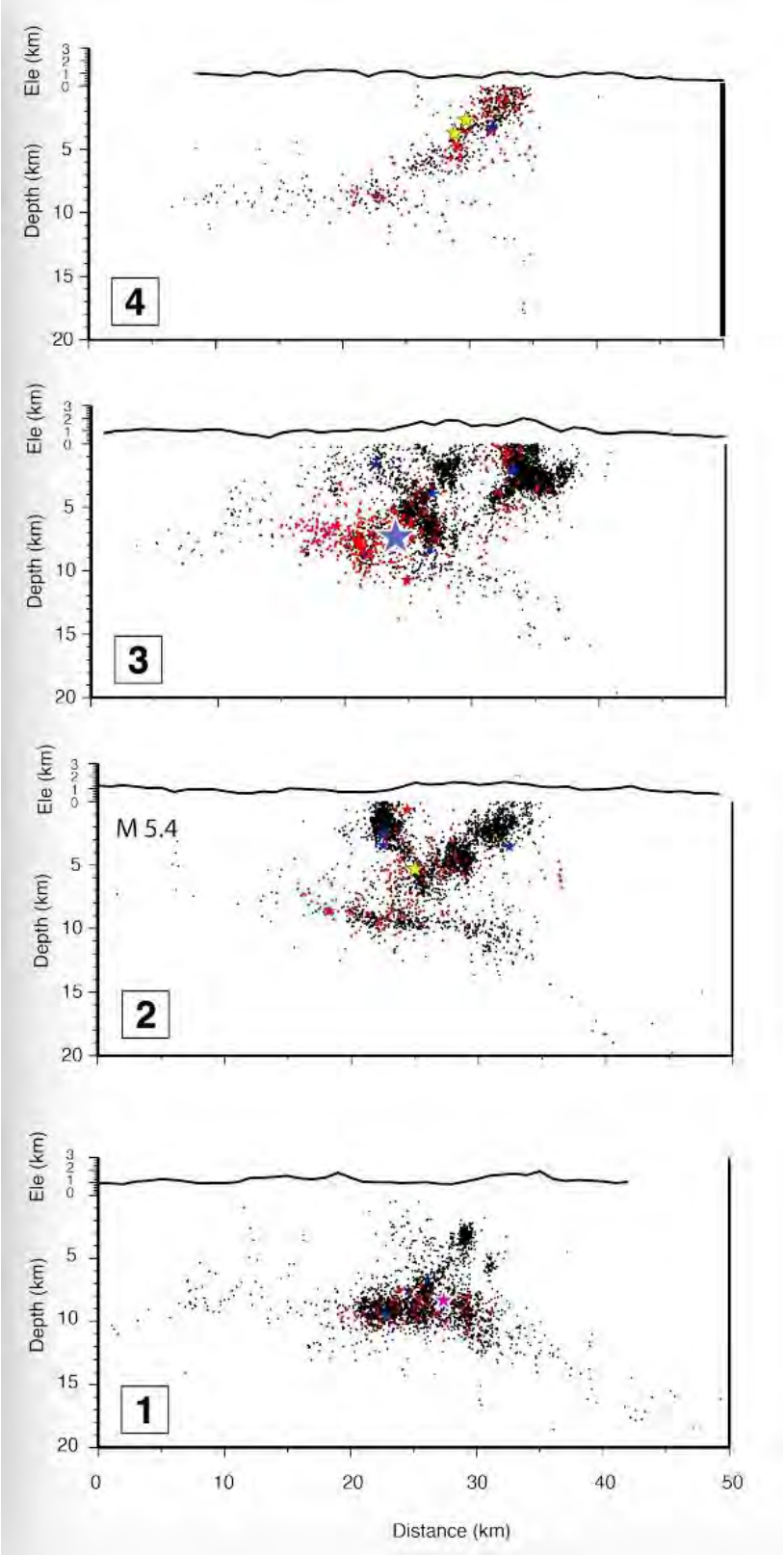

Figure 3.2.2 - Cross sections We observe a main SW-dipping fault plane whose segments show dip angles in between 45-55° varying along strike. All the 3 events with $M_w \geq 5.9$ nucleate along this main plane. In the central portion of the system, in front of the Mt. Vettore structure (sections 2 and 3), we observe the activation of a set of antithetic segments. While going north we have a shallower splay synthetic to the main fault plane and located on its footwall.The entire fault system is constrained at about 7-8 km of depth, by a 2-3 km thick layer, gently dipping to the east.

3.3 Short-term earthquake forecast (OEF) for the Amatrice-Norcia sequence (November 9, 2016)

Following the M6 Amatrice earthquake occurred on August 24, 2016, the seismic hazard center (CPS) at INGV delivered in a pilot testing phase weekly forecasts in a circle area of 50 km around the epicenter (lat. 42.71, lon. 13.22). Since October 26, the area has been increased to a circle with radius of 70 km, and since October 30 the area has been modified considering the zone delimited by the coordinates 42.4N-43.4N, 12.5E- 13.9E. The automatic forecasting procedure has been implemented in the framework of the collaboration between INGV and DPC (allegato B dell'Accordo Quadro DPC-INGV 2012-2021), and it is based on the OEF_Italy model described by Marzocchi et al. (2014). In brief, the model is an ensemble of three different earthquake clustering models that are the best performing in preliminary testing phases carried out by the international network named Collaboratory for the Study of Earthquake Predictability in different regions of the world. The weekly forecasts are updated every week, and after any earthquake of magnitude 4.5 or above.

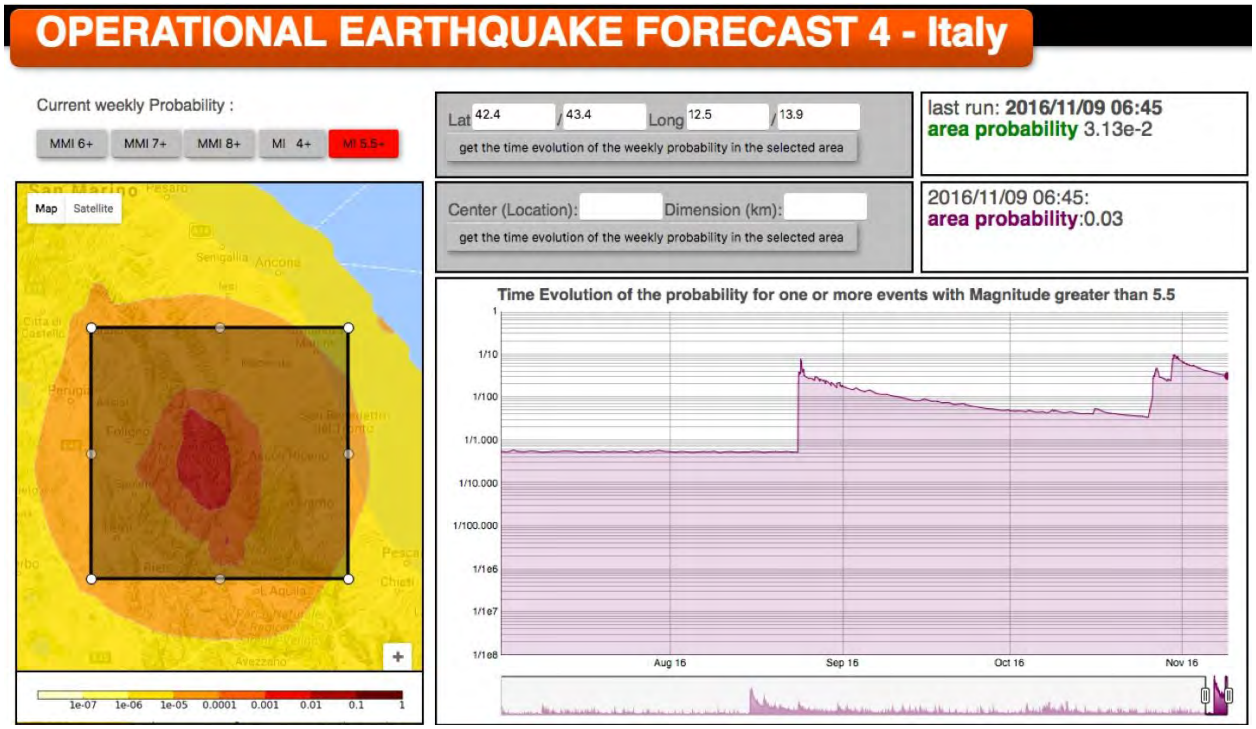

Figure 3.3.1 - The time evolution of the weekly probability of earthquakes with magnitude 5.5 or above in the area reported on the left of the figure.

From the figure showed above we can see that the earthquake occurred on August 24 was not anticipated by any increase in probability (the background probability was about 0.0005), while the weekly probability before the M6.5 occurred on October 30 was about 0.03.

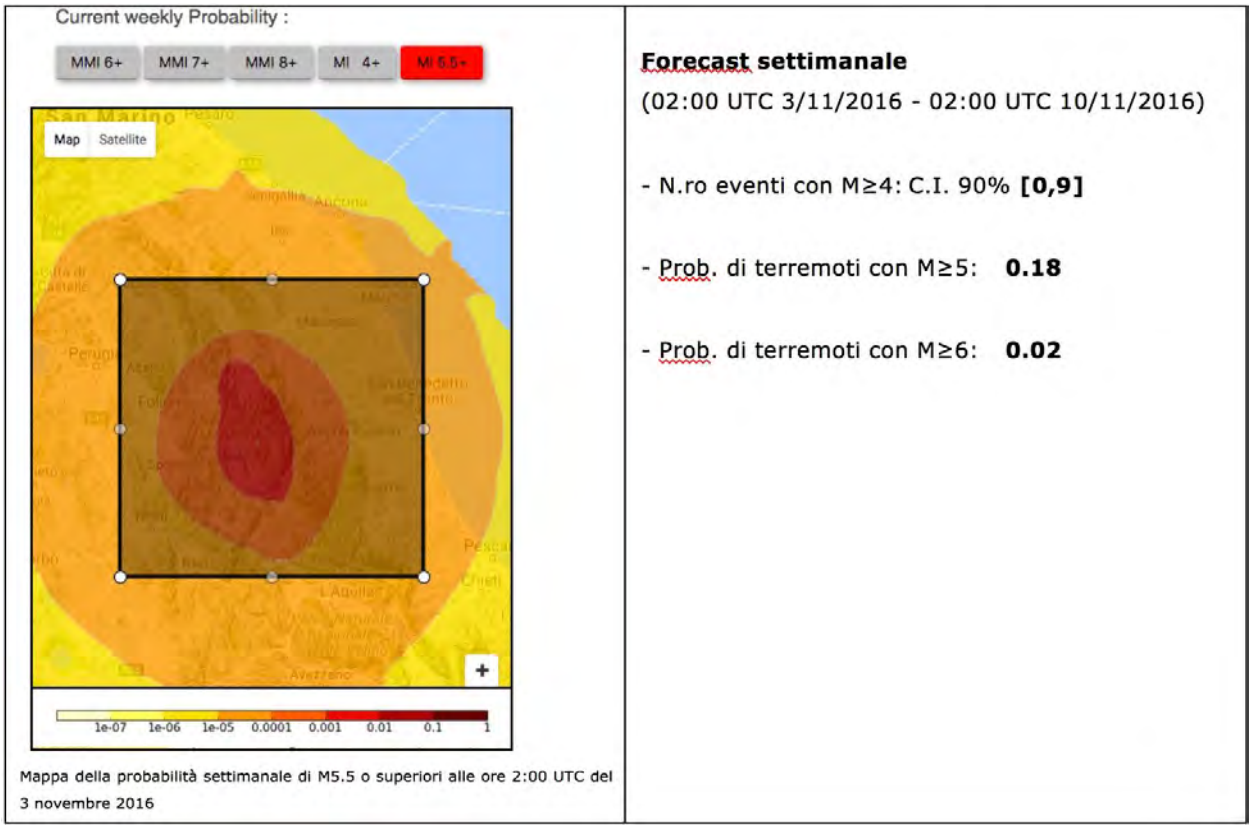

Figure 3.3.2 - The last weekly forecast released on November 3.

References

Akkar, S., M. A. Sandıkkaya, and J. J. Bommer, 2014. Empirical ground-motion models for point- and extended-source crustal earthquake scenarios in Europe and the Middle East, Bull Earthquake Eng, 12(1), 359–387, doi:10.1007/s10518-013-9461-4.

Anzidei, M., P. Baldi, and E. Serpelloni, 2008. The coseismic ground deformations of the 1997 Umbria-Marche earthquakes: A lesson for the development of new GPS networks, Ann. Geophys., 51(2–3), 27– 43.

Barchi M.R., Mirabella F., 2009. The 1997–98 Umbria–Marche earthquake sequence: “Geological” vs.“seismological” faults. Tectonophysics, 476, 170–179.

Bindi, D., F. Pacor, L. Luzi, R. Puglia, M. Massa, G. Ameri, and R. Paolucci, 2011. Ground motion prediction equations derived from the Italian strong motion database, Bull. Earthq. Eng. 9, 1899–1920.

Blumetti A.M., 1995. Neotectonic investigations and evidence of paleoseismicity in the epicentral area of the January-February 1703, Central Italy, earthquakes. In: Serva, L. & Slemmons, D. B., (eds.): Perspectives in paleoseismology. Association of Engineering Geologists, spec. publ. 6, 83-100.

Blumetti A.M., Dramis F., Gentili B., Pambianchi G., 1990. La struttura di M. Alvagnano-Castel Santa Maria nell’area nursina: aspetti geomorfologici e sismicità storica. Rend. Soc. Geol. It., 13, 71-76.

Boncio P., Lavecchia G., Pace B., 2004a. Defining a model of 3D seismogenic sources for Seismic Hazard Assessment applications: the case of central Apennines (Italy). J. Seism., 8, 407–425.

Boncio P., Lavecchia G., Milana G., Rozzi B., 2004b. Improving the knowledge on the seismogenesis of the Amatrice-Campotosto area (central Italy) through an integrated analysis of minor earthquake sequences and structural data. Ann. Geophys. 47, 1723–1742.

Brozzetti F., Lavecchia G., 1994. Seismicity and related extensional stress field; the case of the Norcia seismic zone (central Italy). Annales Tectonicae 8, 36–57.

Cacciuni A., Centamore E., Di Stefano R., Dramis F., 1995. Evoluzione morfotettonica della conca di Amatrice, Studi Geol. Camerti, vol. spec. 1995/2, 95–100.

Calamita F., Pizzi A., 1992. Tettonica quaternaria nella dorsale appenninica umbro-marchigiana e bacini intrappenninici associati. Studi Geologici Camerti, spec. vol. 1992/1, 17-25.

Calamita F., Coltorti M., Deiana G., Dramis F., Pambianchi G., 1982. Neotectonic evolution and geomorphology of the Cascia and Norcia depression (Umbria-Marche Apennine). Geografia Fisica e Dinamica Quaternaria, 5, 263-276.

Calamita F., Pizzi A., Romano A., Roscioni M., Scisciani V., Vecchioni G., 1995. La tettonica quaternaria nella dorsale appenninica umbro-marchigiana: una deformazione progressiva non coassiale. Studi Geol. Camerti, vol. spec.1995/1, 203-223.

Calamita F., Coltorti M., Pieruccini P., Pizzi A., 1999. Evoluzione strutturale e morfogenesi plio-quaternaria dell'appennino umbro-marchigiano tra il preappenino umbro e la costa adriatica. Bollettino della Società Geologica Italiana, 118, 125-139.

Calamita F., Coltorti M., Piccinini D., Pierantoni P.P., Pizzi A., Ripepe M., Scisciani V., Turco E., 2000. Quaternary faults and seismicity in the Umbro-Marchean Apennines (central Italy). Journal of Geodynamics 29, 245–264.

Cello G., Mazzoli S., Tondi E., Turco E., 1997. Active tectonics in the Central Apennines and possible implications for seismic hazard analysis in peninsular Italy. Tectonophysics, 272, 43-68.

Cello G., Deiana G., Mangano P., Mazzoli S., Tondi E., Ferreli L., Maschio L., Michetti A.M., Serva L., Vittori E., 1998. Evidence for surface faulting during the September 26, 1997, Colfiorito (Central Italy) earthquakes. Journal of Earthquake Engineering, 2, 1-22.

Cello G., Deiana G., Ferreli L., Marchegiani L., Maschio L., Mazzoli S., Michetti A., Serva L., Tondi E., Vittori T., 2000. Geological constraints for earthquake faulting studies in the Colfiorito area (central Italy). J. Seismol., 4, 357 – 364.

Chiaraluce, L., Barchi, M., Collettini, C., Mirabella, F., Pucci, S., 2005. Connecting seismically active normal faults with Quaternary geological structures in a complex extensional environment: the Colfiorito 1997 case history (northern Apennines, Italy). Tectonics, 24, TC1002, doi:10.1029/2004TC001627.

Chiarini E., La Posta E., Cifelli F., D'Ambrogi C., Eulilli V., Ferri F., Marino M., Mattei M., Puzzilli L.M., 2014. A multidisciplinary approach to the study of the Montereale Basin (Central Apennines, Italy). Rend. Fis. Acc. Lincei, 25 (Suppl 2), S177–S188. DOI 10.1007/s12210-014-0311-3

Cheloni, D. et al., 2010. Coseismic and initial post-seismic slip of the 2009 Mw 6.3 L'Aquila earthquake, Italy, from GPS measurements, Geophys. J. Int., 181, doi:10.1111/j.1365-246X.2010.04584.x.

Cinti F.R., Cucci L., Marra F., Montone P., 1999. The 1997 Umbria Marche (Italy) earthquake sequence: relationship between ground deformation and seismogenic structure. Geophys. res. Lett., 26, 7, 895-898.

Civico R., Blumetti A.M., Chiarini E., Cinti F.R., La Posta E., Papasodaro F., Sapia V., Baldo M., Lollino G., Pantosti D., 2016. Traces of the active Capitignano and San Giovanni faults (Abruzzi Apennines, Italy). Journal of Maps, http://dx.doi.org/10.1080/17445647.2016.1239229.

Coltorti M., Farabollini P., 1995. Quaternary evolution of the Castelluccio di Norcia Basin. Il Quaternario, 8, 149-166.

De Luca, M. Cattaneo, G. Monachesi, A. Amato (2009) Seismicity in Central and Northern Apennines integrating the Italian national and regional networks. Tectonophysics
Volume 476, Issues 1–2, 15, Pages 121–135

Devoti, R., 2012. Combination of coseismic displacement fields: a geodetic perspective, Ann Geophys-Italy, doi:10.4401/ag-6119.

Galadini F., 2006. Quaternary tectonics and large-scale gravitational deformations with evidence of rock-slide displacements in the central Apennines. Geomorphology, 82, 201-228.

Galadini F., Galli P., 2000. Active tectonics in the Central Apennines (Italy) - Input data for seismic hazard Assessment. Natural Hazards, 22, 225-270.

Galadini F., Messina P., 2001. Plio-Quaternary changes of the normal fault architecture in the central Apennines (Italy). Geodinamica Acta, 14, 321-344.

Galadini F., Galli P., 2003. Paleoseismology of silent faults in the central Apennines (Italy): the Mt. Vettore and Laga Mts. faults. Annali di Geofisica, 46, 815-836.

Galadini F., Galli P., Leschiutta I., Monachesi G., Stucchi M., 1999. Active tectonics and seismicity in the area of the 1997 earthquake sequence in central Italy: a short review. Journal of Seismology, 3, 167-175.

Galli P., Galadini F., Calzoni F., 2005. Surface faulting in Norcia (central Italy): a “paleoseismological perspective”. Tectonophysics, 403, 117-130.

Galvani, A., Anzidei, M., Devoti, R., Esposito, A., Pietrantonio, G., Pisani, A., Riguzzi, F., Serpelloni, E., 2012. The interseismic velocity field of the central Apennines from a dense GPS network. Ann. Geophys. 55, 5, 2012; doi: 10.4401/ag-5634.

Gori S., Dramis F., Galadini F., Messina P., 2007. The use of geomorphological markers in the footwall of active faults for kinematic evaluations: examples from the central Apennines. Bollettino della Società Geologica Italiana, 126, 365-374.

INGV Working group "GPS Geodesy (GPS data and data analysis center)", 2016. Preliminary co-seismic displacements for the August 24, 2016 ML6, Amatrice (central Italy) earthquake from the analysis of continuous GPS stations; https://doi.org/10.5281/zenodo.61355.

Marzocchi W. , A.M. Lombardi, E. Casarotti, 2014. The establishment of an operational earthquake forecasting system in Italy. *Seismol. Res. Lett.*, **85**(5), 961-969

Messina P., Galadini F., Galli P., Sposato A., 2002. Quaternary basin evolution and present tectonic regime in the area of the 1997-98 Umbria-Marche seismic sequence (central Italy). Geomorphology, 42, 97-116.

Pantosti, D., De Martini, P.M., Galli, P., Galadini, F., Messina, P., Moro, M., Sposato, A., 1999. Studi paleosismologici attraverso la rottura superficiale prodotta dal terremoto del 14 ottobre 1997 (Umbria-Marche) Atti 18° Convegno Annuale del G.N.G.T.S., sessione 10 "Forti terremoti dell'area mediterranea".

Paolucci, R., F. Pacor, R. Puglia, G. Ameri, C. Cauzzi, and M. Massa, 2011. Record processing in ITACA, the new Italian strong motion database, in Earthquake Data in Engineering Seismology, Geotech- nical, Geological and Earthquake Engineering Series, S. Akkar, P. Gulkan, and T. Van Eck (Editors), Vol. 14(8), 99–113.

Pizzi A., Scisciani V., 2000. Methods for determining the Pleistocene–Holocene component of displacement on active faults reactivating pre-Quaternary structures: examples from the central Apennines (Italy). Journal of Geodynamics 29, 445–457.

Pizzi A., Galadini F., 2009. Pre-existing cross-structures and active fault segmentation in the northern-central Apennines (Italy). Tectonophysics. 476, 304-319.

Pizzi A., Calamita F., Coltorti M., Pieruccini P., 2002. Quaternary normal faults, intramontane basins and seismicity in the Umbria-Marche- Abruzzi Apennine ridge (Italy): contribution of neotectonic analysis to seismic hazard assessment. Boll. Soc. Geol. It., Spec. Publ., 1, 923–929.

Serpelloni, E. et al., 2012. GPS observations of coseismic deformation following the May 20 and 29, 2012, Emilia seismic events (northern Italy): data, analysis and preliminary models, Ann Geophys., 55(4), doi:10.4401/ag-6168.

Vittori E., Deiana G., Esposito E., Ferreli L., Marchegiani L., Mastrolorenzo G., Michetti A.M., Porfido S., Serva L., Simonelli A.L., Tonoli E., 2000. Ground effects and surface faulting in the September–October 1997 Umbria–Marche (Central Italy) seismic sequence. J. Geod., 29, 535–564.

Disclaimer and limits of use of information

The INGV, in accordance with the Article 2 of Decree Law 381/1999, carries out seismic and volcanic monitoring of the Italian national territory, providing for the organization of integrated national seismic network and the coordination of local and regional seismic networks as described in the agreement with the Department of Civil Protection.
INGV contributes, within the limits of its skills, to the evaluation of seismic and volcanic hazard in the Country, according to the mode agreed in the ten-year program between INGV and DPC February 2, 2012 (Prot. INGV 2052 of 27/2/2012), and to the activities planned as part of the National Civil Protection System.

In particular, this document[1] has informative purposes concerning the observations and the data collected from the monitoring and observational networks managed by INGV.

INGV provides scientific information using the best scientific knowledge available at the time of the drafting of the documents produced; However, due to the complexity of natural phenomena in question, nothing can be blamed to INGV about the possible incompleteness and uncertainty of the reported data.

INGV is not responsible for any use, even partial, of the contents of this document by third parties and any damage caused to third parties resulting from its use.

The data contained in this document is the property of the INGV.

[1] This document is level 3 as defined in the "Principi della politica dei dati dell'INGV (D.P. n. 200 del 26.04.2016)".